Copy 5
RM L54E26

NACA RM L54E26



NACA

# RESEARCH MEMORANDUM

## EFFECT ON DRAG OF LONGITUDINAL POSITIONING OF HALF-SUBMERGED AND PYLON-MOUNTED DOUGLAS AIRCRAFT STORES ON A FUSELAGE WITH AND WITHOUT CAVITIES BETWEEN MACH NUMBERS 0.9 AND 1.8

By Sherwood Hoffman and Austin L. Wolff

Langley Aeronautical Laboratory







NATIONAL ADVISORY COMMITTEE FOR AERONAUTICS

WASHINGTON

July 15, 1954

NACA RM L54E26



NATIONAL ADVISORY COMMITTEE FOR AERONAUTICS

RESEARCH MEMORANDUM

# EFFECT ON DRAG OF LONGITUDINAL POSITIONING OF HALF-SUBMERGED AND PYLON-MOUNTED DOUGLAS AIRCRAFT STORES ON A FUSELAGE WITH AND WITHOUT CAVITIES BETWEEN MACH NUMBERS 0.9 AND 1.8

By Sherwood Hoffman and Austin L. Wolff

## SUMMARY

The effect on drag of positioning symmetrically mounted Douglas Aircraft Company, Inc. stores in pairs on a parabolic fuselage of fineness ratio 10.0 has been determined by flight tests of rocket-propelled, zero-lift models through a range of Mach number from 0.9 to 1.8. The stores were mounted in half-submerged positions and on pylons and were tested in three longitudinal locations on the fuselage with the forward position being located at the maximum diameter of the fuselage. The effects on drag of removing the half-submerged stores or extending them outward on pylons also was investigated by tests of models with half-submerged-store cavities on the fuselage. Two pylons differing in airfoil section and thickness were tested at the forward position of the stores on the fuselage with cavities.

The half-submerged stores gave the smallest drag increments, which were approximately equal regardless of their respective longitudinal locations. Removing the half-submerged stores to expose the cavities increased the drag increments from two to three times. For the pylon-mounted stores, the store in the midposition had less drag than in the forward or rear positions at supersonic speeds. Adding the half-submerged-store cavities to the pylon-mounted-store configurations reduced the drag at the rear position between Mach numbers 0.95 and 1.50 and increased the drag at the midposition throughout the speed range. Changing from the 6-percent-thick flat pylon to the 10-percent-thick airfoil pylon increased the total drag slightly above Mach number 1.10. Good agreement was obtained between the experimental and theoretical interference drag coefficients for the pylon-mounted stores (without fuselage cavities) in the three longitudinal locations tested at Mach numbers 1.2 and 1.5.

[redacted]

## INTRODUCTION

The arrangement of the various components of an aircraft may produce large unfavorable interference effects at transonic and supersonic speeds. In order to prevent or eliminate such unfavorable interference, a general study of interference is being made by using concepts based on the transonic area rule and linearized theory. Owing to the complex nature of the problem, it was found convenient to use simplified configurations for studying the basic problem of interference on the premise that the findings will be useful in analyzing interference problems of complete aircraft.

Recent investigations (refs. 1 and 2) of store-fuselage combinations without wings show that the position of the store or bomb is important from the considerations of drag, buffet, trim, and release characteristics at high speeds. Reference 3 presents a theoretical study of interference effects for special bodies of revolution in various arrangements at supersonic speeds and shows that the interference drag is dependent on the relative position of the stores in combination with the fuselage. The present paper shows the effect on interference drag of locating symmetrically mounted Douglas Aircraft Company, Inc., stores in pairs on a parabolic fuselage without wings and presents a study of the resulting interference effects based on the concepts of the transonic area rule and linearized theory. Pylon-mounted and half-submerged stores were tested in three longitudinal positions on the fuselage, the forward position being located at the maximum diameter of the fuselage. The effect on drag of removing the half-submerged stores or extending them outward on pylons and thus leaving half-submerged-store cavities exposed were investigated also at the three longitudinal positions.

All the configurations were rocket-propelled, zero-lift models and were tested at the Langley Pilotless Aircraft Research Station at Wallops Island, Va. The flight tests covered a continuous speed range with Mach numbers varying from about 0.9 to 1.8 and Reynolds numbers from approximately $20 \times 10^6$ to $60 \times 10^6$, based on the length of the models.

## SYMBOLS

| | |
|---|---|
| $A$ | cross-sectional area, sq in. |
| $a$ | tangential acceleration, ft/sec |
| $C_D$ | total drag coefficient based on $S_f$ |

[redacted]

| | |
|---|---|
| $C_{D_S}$ | drag coefficient of isolated store based on $S_S$ |
| $C_{D_I}$ | interference drag coefficient based on $S_s$ |
| $C_p$ | pressure coefficient |
| $C_{p_I}$ | interference pressure coefficient |
| c | pylon chord, in. |
| g | acceleration due to gravity, $ft/sec^2$ |
| L | length of fuselage, in. |
| $l$ | length of store, in. |
| M | Mach number |
| $Q_i$ | pressure function |
| q | dynamic free-stream pressure, lb/sq ft |
| $R_e$ | Reynolds number |
| r | radius, in. |
| $r_o$ | distance between center lines of store and fuselage, in. |
| $S_f$ | frontal area of fuselage, sq ft |
| $S_S$ | frontal area of isolated store, sq ft |
| $S_s$ | frontal area of one store on fuselage, sq ft |
| t | thickness of pylon, in. |
| W | weight of model during deceleration, lb |
| $\gamma$ | angle between flight path and horizontal, deg |
| x | longitudinal station, in. |
| X | distance between center of gravity of store and nose of fuselage, in. |

[redacted]

$\beta = \sqrt{M^2 - 1}$

$\xi$ abscissa of source or sink along x-axis

## MODELS

A list of the models tested and their identifying symbols are given in table I. Details and dimensions of the parabolic fuselage, the stores, the pylons, and the store-fuselage combinations are presented in figures 1 to 3 and tables II to VI. The cross-sectional-area distributions and photographs of the models showing close-up views of the stores, pylons, and cavities are given in figures 4 and 5, respectively.

The fuselage consisted of two parabolas of revolution joined at the maximum diameter (40-percent station) and had an overall fineness ratio of 10. Four thin 60° sweptback fins with beveled leading and trailing edges were used to stabilize this body in flight.

The Douglas Aircraft store shape (fineness ratio 8.57) with fins C of reference 4 was selected for the tests. The stores mounted on the fuselage were 18 inches long or 0.10 full scale for the 150-gallon Douglas Aircraft store. The isolated store, which was 0.33 full scale or 60 inches long, was modified slightly at two stations on the afterbody (fig. 2(b)) in order to fit the booster-rocket-motor adaptor.

The store-fuselage combinations consisted of pylon-mounted stores with and without half-submerged-store cavities in the fuselage, half-submerged stores, and half-submerged-store cavities alone in the fuselage. The stores, pylons, and cavities were mounted symmetrically in pairs on the fuselage as is shown in figure 3. The minimum distance between the pylon-mounted stores and fuselage surface without cavities was kept constant at 0.7 inch to allow for fin clearance (fig. 2(a)) as the longitudinal location of the stores was varied. The half-submerged stores had three fins exposed, two of the fins being tangent to the fuselage surface (fig. 5(c)).

The stores, pylons, and cavities were located in three longitudinal locations on the fuselage which will be referred to as the forward, middle, and rear locations. These locations, based on the distance X between the center of gravity of the stores and the nose of the fuselage, are at the 0.40, 0.525, and 0.65 stations of the fuselage. No locations were tested forward of the maximum-diameter station of the fuselage.

Two pylon sections differing in shape and thickness were used for the present tests. The 6-percent-thick section had a flat midsection with an elliptical leading edge and wedge-shaped trailing edge. This

pylon is similar to the Douglas 3-hook shackle pylon of reference 5. The 10-percent-thick pylon, which was tested only in the forward position, was similar to that used in reference 4.

## TESTS AND MEASUREMENTS

The rocket-propelled zero-lift models were tested at the Langley Pilotless Aircraft Research Station at Wallops Island, Va. Each model was boosted from a zero-length launcher (fig. 6) to supersonic speeds by a fin-stabilized 6-inch ABL Deacon rocket motor. All the models except model N, the isolated store, had a 2.25-inch aircraft rocket motor included in the fuselage for additional propulsion. The models were tracked by a CW Doppler velocimeter and an NACA modified SCR 584 radar tracking unit to determine the deceleration and trajectory during coasting flight. A survey of atmospheric conditions was made by radiosonde measurements from an ascending balloon that was released at the time of each launching.

The flight tests covered continuous ranges of Mach number varying from about 0.9 to 1.8 and Reynolds numbers from approximately $20 \times 10^6$ to $60 \times 10^6$, based on the length of the models, as is shown in figure 7.

The values of total drag coefficient, based on the frontal area of the parabolic fuselage, for models A to M and the fuselage alone was obtained from the expression

$$C_D = \frac{-W}{gqS_f}(a + g \sin \gamma)$$

The drag coefficient of two isolated stores, based on the fuselage frontal area, is

$$C_{D_{stores}} = 2C_{D_S}\frac{S_s}{S_f}$$

where $C_{D_S}$ is based on the frontal area of the isolated store tested.

The interference drag coefficient based on the frontal area of the stores was determined for models A to C by subtracting the drags of the isolated stores, pylons, and fuselage from the total drag or

[redacted]

$$C_{D_I} = \left(C_D - C_{D_{fuselage}}\right)\frac{S_f}{2S_s} - C_{D_S} - C_{D_{pylon}}$$

where the drag coefficient of the pylon is based on the frontal area of the store. The drag of the 6-percent-thick pylon was estimated by using two-dimensional theory at supersonic speeds with an allowance for the blunt leading edge. The drag from the 10-percent-thick pylon was estimated from the flight-test data of reference 6.

The error in total drag coefficient was estimated to be approximately ±0.005 at supersonic speeds and ±0.01 at subsonic and transonic speeds. The Mach numbers were determined within ±0.005.

## RESULTS AND DISCUSSION

The variations of the drag coefficients $C_D$ and $C_{D_S}$ with Mach number for the parabolic fuselage and isolated store are presented in figures 8(a) and 8(b), respectively. At supersonic speeds, the store has a greater drag coefficient than the fuselage because of its body shape and lower fineness ratio. However, at subsonic speeds the fuselage has the greater drag coefficient because of the base drag and greater wetted area, especially from the fins. The amount of drag due to the modification on the afterbody of the isolated store (fig. 2(b)) was not determined, but it is believed to be negligible.

The effect on drag of varying the longitudinal position of the stores, pylons, and cavities on the fuselage is shown in figure 9. The drag of two isolated stores, based on the fuselage frontal area, is presented also in figure 9 for comparison with the drag increments from the stores and cavities. The estimated drags of the 6-percent-thick and 10-percent-thick pylons are shown in figure 9(a) to be small relative to the total drag of the configuration and of the order of accuracy of the tests.

The pylon-mounted stores (fig. 9(a)) increased the drag of the fuselage by an amount that is either equal to or greater than the drag of two isolated stores and pylons. The largest drag increments for the pylon stores were obtained in the forward position (X/L = 0.40), where the maximum cross-sectional areas of the fuselage and stores are alined. Owing to the failure of a flight model that utilized the 6-percent-thick pylon in the forward position, only the data from the 10-percent-thick pylon in the forward position are available for presentation in figure 9(a). However, changing from the 6-percent-thick pylon to the 10-percent-thick

pylon probably would have a small effect on the total drag since the drag from the two pylons was estimated to be small. The drag increments from the stores on the 6-percent-thick pylon at the middle position ($X/L = 0.525$) were the smallest obtained from the pylon-mounted stores without cavities at supersonic speeds and were approximately equal to the drags of the isolated stores and pylons throughout most of the test range.

When the pylon-mounted stores were tested with the half-submerged-store cavities on the fuselage, the rear installation had considerably lower drag increments than were obtained at the forward and middle positions throughout the Mach number range as is shown in figure 9(b). The drag from the stores, pylons, and cavities at $X/L = 0.65$ was approximately equal to the sum of the drags of the isolated stores and pylons; therefore, no unfavorable interference effects from the rear cavities was indicated at supersonic speeds. Changing from the 6-percent-thick pylon to the 10-percent-thick pylon at $X/L = 0.40$ resulted in a small increase in the total drag above $M = 1.1$. The forward stores on both pylons tested and the middle stores experienced a large increase in subsonic drag because of the cavities.

The half-submerged stores gave the smallest drag increments without any significant effects resulting from changing their longitudinal positions at supersonic speeds (fig. 9(c)). The drags from these half-submerged stores with three fins exposed were less than half the drag of the isolated stores above Mach number 1.05; this result indicates a small amount of favorable interference effects at supersonic speeds. It should be noted, however, that this savings in drag was obtained at the cost of reducing the total volume of the configuration by approximately one-half the volume of the stores. Near Mach number 1.0 and at subsonic speeds the drag from the half-submerged stores at $X/L = 0.65$ was significantly less than that from the stores at the forward and middle positions.

The drag increments from the cavities alone are shown in figure 9(d) to be large in the three longitudinal locations tested and of the same order of magnitude as that from the isolated stores at supersonic speeds. Near Mach number 1.0, the drag increment from the cavities in the middle position was approximately twice as large as the drag increment from the cavities in either the forward or rear location. Unpublished data indicate that the drag from the cavities was due mainly to a localized effect caused by turbulence within the cavities.

Figure 10 is presented in order to show more clearly the effects on drag of moving the half-submerged stores outward on the pylons or removing the half-submerged stores at each longitudinal position tested. Removing the half-submerged stores and exposing the cavities increased the drag increments to two to three times those of the half-submerged stores throughout most of the speed range at each longitudinal location. When

the half-submerged stores were extended vertically on pylons and the cavities left open, the drag increments were increased from four to five times that of the half-submerged stores at supersonic speeds. Closing the cavities reduced the drag coefficient of the pylon-mounted stores at $X/L = 0.525$ by 0.025 throughout the test range and increased the drag of the pylon-mounted stores at $X/L = 0.65$ between Mach numbers 0.95 and 1.5. At the forward position $X/L = 0.40$, the cavities had a negligible effect on the drag of the pylon-mounted stores above Mach number 1.0 and a large unfavorable effect at subsonic speeds.

The drag-rise Mach numbers varied between $M = 0.93$ and 0.97, the lowest drag-rise Mach numbers being obtained from the configurations having the highest drag rises.

A comparison of the maximum drag rises of the configurations tested is presented in figure 11 in order to determine whether the transonic area rule (ref. 7) can be applied to a comparison of the drag rises of combinations of bodies without wings, such as those of the present investigation. The area rule of reference 7 states that the zero-lift drag rise of thin, low-aspect-ratio, wing-body combinations near the speed of sound is primarily dependent on the axial distribution of cross-sectional areas normal to the axis of symmetry. References 8 and 9, for example, show that the area rule may be extended to wing-body combinations with external stores or nacelles to a limited extent. A comparison of the area distributions in figure 4 with the results in figure 11 shows that the highest drag rises were obtained from the configurations with the pylon-mounted stores, which gave the largest rate of increase of cross-sectional area in each longitudinal position tested. Adding the fuselage cavities to the configurations with the pylon-mounted stores reduced the rate of development of the areas somewhat and lowered the drag rises. Although the indentation produced by the cavities of models D, E, F, and M was localized, it produced a similar effect in reducing the drag rise as was obtained with symmetrical indentations in reference 7 and two-dimensional indentations in reference 10 and unpublished data. The changes in area development resulting from the half-submerged stores or cavities alone were smaller than those for the pylon stores and caused little or no changes in the total drag rises. As is indicated in figure 11, the area rule does not apply when the store, pylon, and cavity installations are varied longitudinally even though there is a noticeable change in the area development of the configurations. A possible explanation for this phenomenon is given in reference 11, which indicates that small changes in the total-area distribution of a configuration generally result in interference effects that are independent of the longitudinal location of the change near and above Mach number 1.0.

The applicability of the linearized theory of reference 3 for determining the interference effects at supersonic speeds for external-store—fuselage combinations was investigated by calculating the interference drags for the pylon-mounted stores without cavities (models A, B, and C)

and comparing the results with the experimental interference drags at Mach numbers 1.2 and 1.5. The theoretical interference drags were obtained entirely by graphical procedures and the method used is outlined in the appendix. The comparison in figure 12 shows that reasonably good agreement was obtained between the theoretical and experimental values of interference drag coefficient at each longitudinal location of the stores. The theoretical values represent the sum of the interference drags from the principal components of the configuration or the total effect of the stores on the fuselage, the fuselage on the stores, and the stores on each other. Figure 13 shows these individual effects at Mach numbers 1.2 and 1.5. Theoretically, the effect of the fuselage on the stores produced the largest variation in the interference drag coefficient as the store location was varied longitudinally. The same method of calculation was used for the half-submerged stores and the results indicated relatively large values of unfavorable interference which were contrary to the experimental results. However, the theory appears to be applicable for external-store installations on pylons without cavities for configurations that are similar to those of the present tests.

## CONCLUSIONS

The effect on drag of the longitudinal positioning of half-submerged and pylon-mounted stores in symmetrical arrangements on a parabolic fuselage with and without half-submerged-store cavities has been determined by flight tests of zero-lift, rocket-propelled models between Mach numbers of 0.9 and 1.8. The centers of gravity of the stores were located at the 0.40, 0.525, and 0.65 stations of the fuselage for the tests. The following conclusions were indicated:

1. The half-submerged stores gave the lowest drag increments, which were approximately the same in the three longitudinal positions tested. Removing the half-submerged stores to expose the cavities increased the drag increments to two to three times those of the half-submerged stores.

2. For the pylon-mounted stores, the store in the middle position had less drag than in the forward or rear positions at supersonic speeds. Adding the half-submerged-store cavities to the fuselages of these configurations reduced the drag at the rear position between Mach numbers 0.95 and 1.50 and increased the drag at the middle position throughout the speed range.

3. Changing from the 6-percent-thick flat pylon to the 10-percent-thick airfoil pylon on the configuration with the pylon stores and cavities in the forward location increased the total drag slightly at Mach numbers above 1.10.

[redacted]

4. Good agreement was obtained between the experimental and theoretical interference drag coefficients for the configurations with the pylon-mounted stores located in the three longitudinal locations tested at Mach numbers 1.2 and 1.5.

Langley Aeronautical Laboratory,
National Advisory Committee for Aeronautics,
Langley Field, Va., May 13, 1954.

[redacted]

## APPENDIX

## METHOD OF CALCULATION

Reference 3 presents an analytical study of interference drags for special bodies of revolution in various two-body and three-body combinations at supersonic speeds. In order to apply the linearized theory of reference 3 to arbitrary body shapes, such as those used herein, it was found convenient to use the rapid graphical method of reference 12 for determining the interference pressures. For the arrangement of bodies of this investigation, each body was entirely or partially immersed in the flow fields of the other bodies throughout the range of flight Mach numbers. When the linearized assumptions of reference 3 were used, the interference pressures acting on each body were taken directly from the pressure fields of the neighboring bodies. Thus, the mutual effects of the principal components of the configuration on interference were determined. In the present analysis, the effects of the store fins and the pylons on the interference drag is not considered.

The rapid graphical method in reference 12 was used therein to determine the pressure distribution on slender, arbitrary bodies of revolution. However, this method may be used also to obtain the flow-field pressures of the arbitrary bodies in a simple way. According to reference 12, the pressure coefficient at any point $x$ on the surface of the body as obtained by the method of sources and sinks is

$$C_{p_x} = \sum_{i=1}^{i=n} \frac{2Q_i}{\sqrt{(x - \xi_i)^2 - (\beta r_x)^2}} \tag{A1}$$

where

$$Q_i = \frac{\Delta\left(r \frac{dr}{dx}\right)\Delta x}{\Delta x/2} \tag{A2}$$

and $n$ is the number of point sources on the body axis. The values of the pressure function $Q_i$ for each $n$ is determined graphically from the shape of the body. In order to calculate the pressures in the flow field of the body and at a constant distance from the center line, the values of $r_x$ in equation (A1) are kept constant. For the present

[redacted]

configurations, $r_x$ was made equal to $r_o$ or $2r_o$, depending on the distance between the center lines of the fuselage and stores or between the stores of the combination. The pressure distributions induced by each body were obtained by evaluating each of 20 sources and sinks along the body axis and summing them in the same manner as is described in reference 12. The pressures induced from the nose of each body were determined by considering the nose to be conical and to have an attached, oblique shock.

The interference pressure drag coefficient for each body was obtained by integrating the interference pressures from the surrounding flow fields about the body by using, for example, the expression

$$C_{D_{I\text{one body}}} = \frac{2}{r_{max}^2} \int_0^l C_{p_I} r \frac{dr}{dx} dx \qquad (A3)$$

which was evaluated graphically. The total interference drag coefficient, according to the linearized assumptions (ref. 3), was obtained by adding the individual interference drag coefficients from each body in the combination.

The interference pressure distributions acting on the fuselage and stores of models A, B, and C were calculated at Mach numbers 1.2 and 1.5 for an average value of $r_o$ of 5.0 inches and are presented in figures 14 to 16. The value of $r_o$ actually varied slightly as the store position was varied longitudinally (fig. 3), but the magnitude of change in $r_o$ was small enough to be neglected without affecting the theoretical pressures in the flow field. The resulting interference drag coefficients, based on the frontal area of the stores, of the principal components of the configuration are shown in figure 13.

[redacted]

## REFERENCES


1. Mason, Homer P.: Effects of External Store Mounting on the Buffet, Trim, and Drag Characteristics of Rocket-Powered Fuselage and Store Combinations Between Mach Numbers of 0.7 and 1.4. NACA RM L53J22, 1953.

2. Rainey, Robert W.: A Wind-Tunnel Investigation of Bomb Release at a Mach Number of 1.62. NACA RM L53L29, 1954.

3. Friedman, Morris D.: Arrangement of Bodies of Revolution in Supersonic Flow To Reduce Wave Drag. NACA RM A51I20, 1951.

4. Muse, T. C., and Kasri, E. B.: Wind Tunnel Tests of the Douglas Aircraft Store With Various Fins. Rep. No. ES 21198, Douglas Aircraft Co., Inc., July 15, 1948.

5. Dugan, James C.: External Store Development. Memo. Rep. No. WCNSR-43019-1-1, Wright Air Dev. Center, U. S. Air Force, Aug. 13, 1951.

6. Tucker, Warren A., and Nelson, Robert L.: Drag Characteristics of Rectangular and Swept-Back NACA 65-009 Airfoils Having Various Aspect Ratios as Determined by Flight Tests at Supersonic Speeds. NACA RM L7C05, 1947.

7. Whitcomb, Richard T.: A Study of the Zero-Lift Drag-Rise Characteristics of Wing-Body Combinations Near the Speed of Sound. NACA RM L52H08, 1952.

8. Hoffman, Sherwood, and Pepper, William B., Jr.: The Effect of Nacelle Combinations and Size on the Zero-Lift Drag of a 45° Sweptback Wing and Body Configuration as Determined by Free-Flight Tests at Mach Numbers Between 0.8 and 1.3. NACA RM L53E25, 1953.

9. Smith, Norman F., Bielat, Ralph P., and Guy, Lawrence D.: Drag of External Stores and Nacelles at Transonic and Supersonic Speeds. NACA RM L53I23b, 1953.

10. Pepper, William B.: The Effect on Zero-Lift Drag of an Indented Fuselage or a Thickened Wing-Root Modification to a 45° Sweptback Wing-Body Configuration as Determined by Flight Tests at Transonic Speeds. NACA RM L51F15, 1951.

11. Jones, Robert T.: Theory of Wing-Body Drag at Supersonic Speeds. NACA RM A53H18a, 1953.


[redacted]

12. Thompson, Jim Rogers: A Rapid Graphical Method for Computing the Pressure Distribution at Supersonic Speeds on a Slender Arbitrary Body of Revolution. NACA TN 1768, 1949.

[redacted]

TABLE I.- MODELS TESTED

| Model | Description | t/c of pylon | X/L |
|---|---|---|---|
| A | Store + pylon | 0.10 | 0.40 |
| B | Store + pylon | .06 | .525 |
| C | Store + pylon | .06 | .65 |
| D | Store + pylon + cavity | .06 | .40 |
| E | Store + pylon + cavity | .06 | .525 |
| F | Store + pylon + cavity | .06 | .65 |
| G | Half-submerged store | ---- | .40 |
| H | Half-submerged store | ---- | .525 |
| I | Half-submerged store | ---- | .65 |
| J | Cavity | ---- | .40 |
| K | Cavity | ---- | .525 |
| L | Cavity | ---- | .65 |
| M | Store + pylon + cavity | .10 | .40 |
| N | Isolated store | ---- | ----- |
| O | Fuselage alone | ---- | ----- |

[redacted]

TABLE II.- COORDINATES OF PARABOLIC FUSELAGE

[Station measured from fuselage nose]

| Station, in. | Ordinate, in. |
|---|---|
| 0 | 0 |
| 1 | .245 |
| 2 | .481 |
| 4 | .923 |
| 6 | 1.327 |
| 10 | 2.019 |
| 14 | 2.558 |
| 18 | 2.942 |
| 22 | 3.173 |
| 26 | 3.250 |
| 30 | 3.233 |
| 34 | 3.181 |
| 38 | 3.095 |
| 42 | 2.975 |
| 46 | 2.820 |
| 50 | 2.631 |
| 54 | 2.407 |
| 58 | 2.149 |
| 62 | 1.857 |
| 65 | 1.615 |

[redacted]

TABLE III.- COORDINATES FOR 18-INCH STORE

[Station measured from store nose]

| Station, in. | Ordinate, in. |
|---|---|
| 0 | 0 |
| .35 | .170 |
| .85 | .366 |
| 1.35 | .517 |
| 1.85 | .633 |
| 2.35 | .723 |
| 2.85 | .795 |
| 3.85 | .905 |
| 4.85 | .987 |
| 5.85 | 1.041 |
| 7.65 | 1.050 |
| 9.45 | 1.046 |
| 10.45 | 1.016 |
| 11.45 | .960 |
| 12.45 | .880 |
| 13.45 | .780 |
| 14.45 | .665 |
| 15.45 | .538 |
| 16.45 | .404 |
| 17.25 | .293 |
| 17.65 | .217 |
| 18.00 | 0 |
| Trailing-edge radius, 0.100 | |

TABLE IV.- COORDINATES FOR 60-INCH ISOLATED STORE

[Station measured from store nose]

| Station, in. | Ordinate, in. |
|---|---|
| 0 | 0 |
| 1.164 | .576 |
| 2.502 | 1.101 |
| 3.834 | 1.536 |
| 5.166 | 1.887 |
| 7.836 | 2.409 |
| 10.500 | 2.772 |
| 13.164 | 3.048 |
| 15.834 | 3.267 |
| 18.498 | 3.429 |
| 21.150 | 3.500 |
| 29.802 | 3.500 |
| 32.502 | 3.468 |
| 35.166 | 3.372 |
| 37.836 | 3.222 |
| 39.162 | 3.126 |
| 41.832 | 2.901 |
| 44.502 | 2.634 |
| 47.166 | 2.334 |
| 49.836 | 2.007 |
| 52.500 | 1.659 |
| 55.164 | 1.302 |
| 56.164 | 1.167 |
| 57.498 | .978 |
| 58.836 | .726 |
| 60.000 | 0 |
| Trailing-edge radius, 0.325 | |

[redacted]

TABLE V.- COORDINATES OF 6-PERCENT-THICK PYLON SECTION

[Station measured from leading edge]

| Station, in. | Ordinate, in. |
|---|---|
| 0 | 0 |
| .005 | .016 |
| .020 | .030 |
| .060 | .051 |
| .100 | .065 |
| .200 | .090 |
| .400 | .120 |
| .600 | .137 |
| .800 | .147 |
| 1.001 | .150 |
| 3.751 | .150 |
| 5.000 | 0 |
| Trailing-edge radius, 0.019 | |

[redacted]

TABLE VI.- COORDINATES OF 10-PERCENT-THICK PYLON SECTION

[Station measured from leading edge]

| Station, in. | Ordinate, in. |
|---|---|
| 0 | 0 |
| .050 | .050 |
| .100 | .070 |
| .250 | .110 |
| .500 | .155 |
| 1.001 | .205 |
| 1.501 | .235 |
| 2.002 | .248 |
| 2.252 | .250 |
| 2.752 | .242 |
| 3.253 | .215 |
| 3.753 | .170 |
| 4.253 | .105 |
| 4.754 | .035 |
| 5.000 | 0 |
| Trailing-edge radius, 0.003 | |

[redacted]

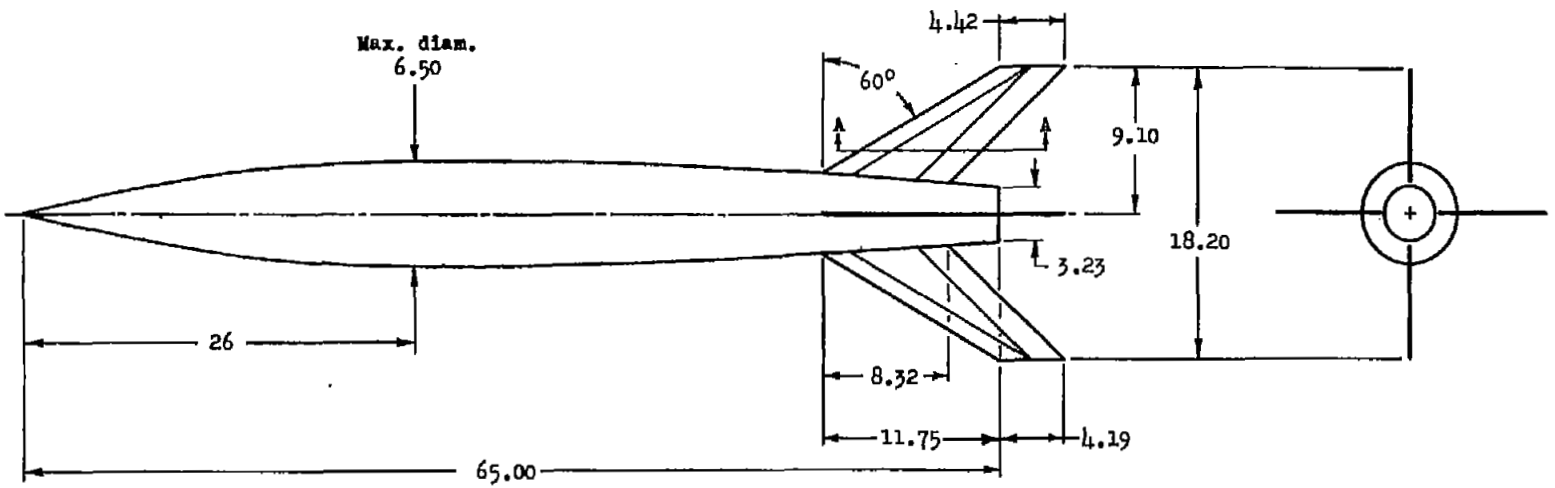


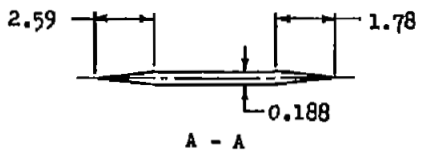


Typical fin section

Fuselage fineness ratio = 10
Fuselage frontal area = 0.230 sq ft

Figure 1.- Details and dimensions of parabolic fuselage. All dimensions are in inches.

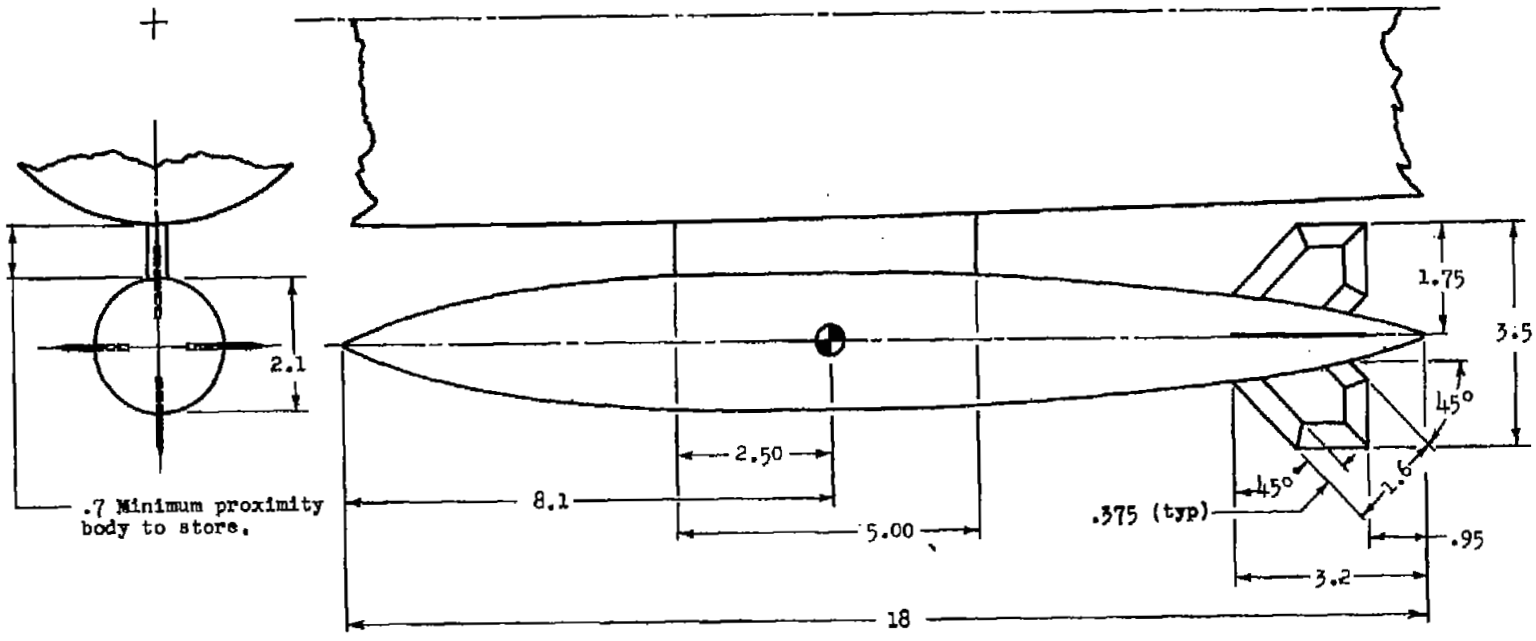


Fineness ratio = 8.57
Frontal area = 0.024 sq ft

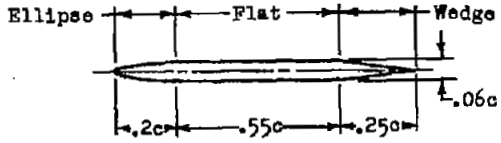


Airfoil shape of t/c=.06 pylon.

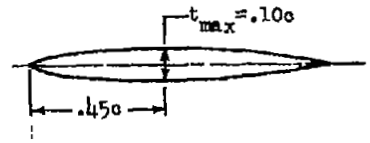


Airfoil shape of t/c=.10 pylon.

(a) Pylon-mounted store.

Figure 2.- Detail and dimensions of stores. All dimensions are in inches.

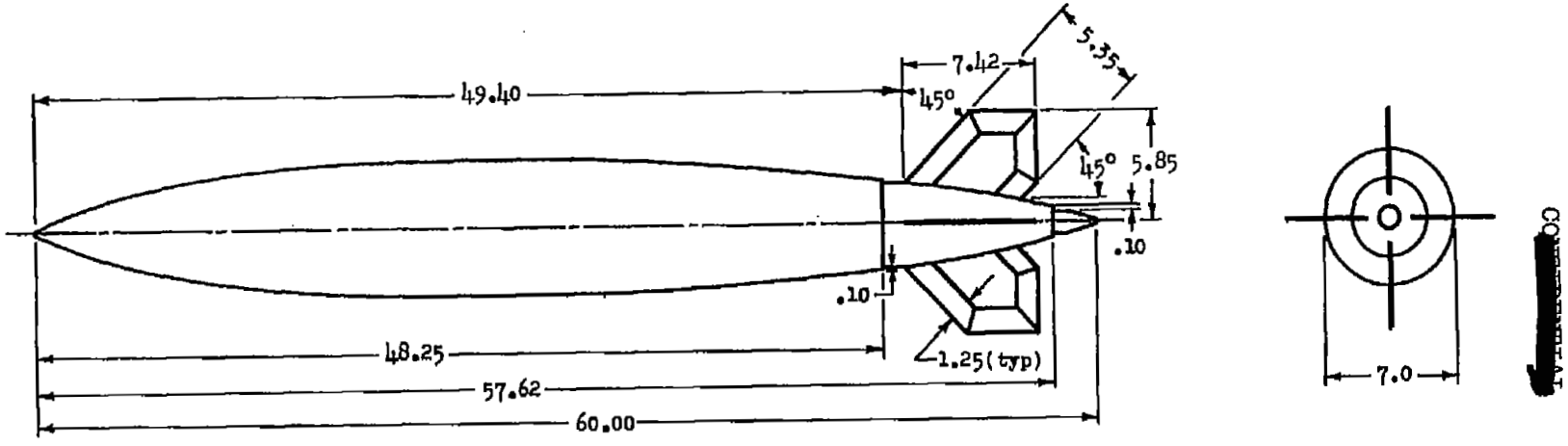


Fineness ratio = 8.57
Frontal area = 0.214 sq ft

(b) Isolated store.

Figure 2.- Concluded.

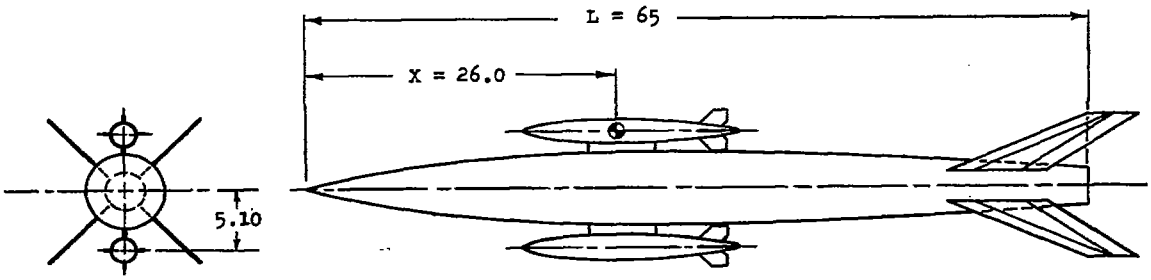


(a) Model A. Stores at X/L = 0.40 and pylon t/c = 0.10.

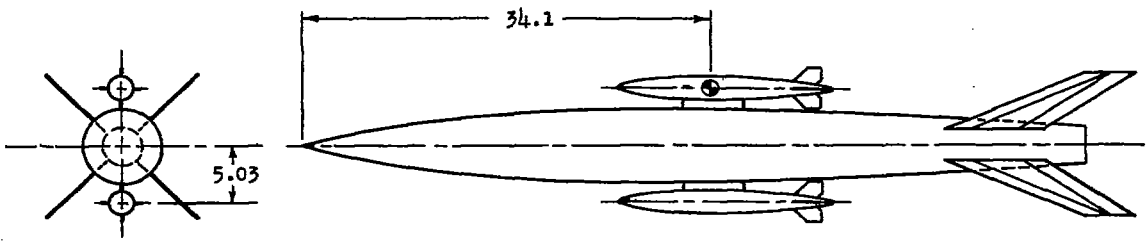


(b) Model B. Stores at X/L = 0.525 and pylon t/c = 0.06.

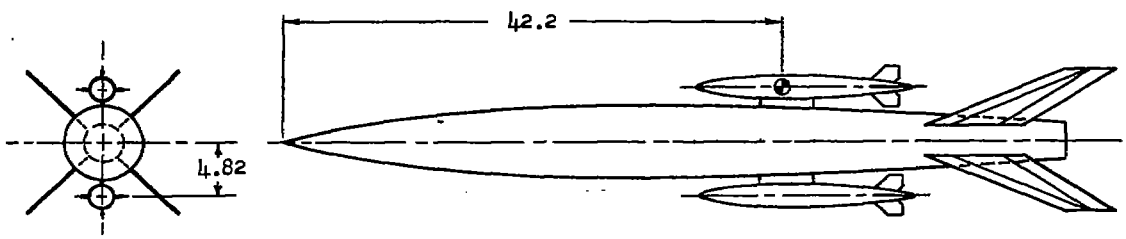


(c) Model C. Stores at X/L = 0.65 and pylon t/c = 0.06.

Figure 3.- Details of store and cavity arrangements on models tested. All dimensions are in inches.

[redacted]

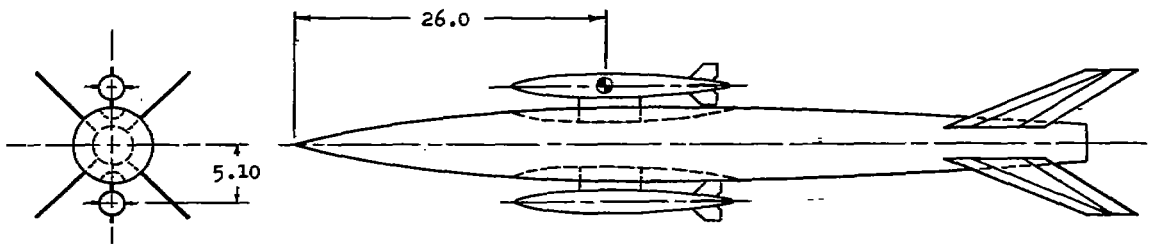


(d) Model D. Stores and cavities at X/L = 0.40 and pylon t/c = 0.06.
Model M. Stores and cavities at X/L = 0.40 and pylon t/c = 0.10.

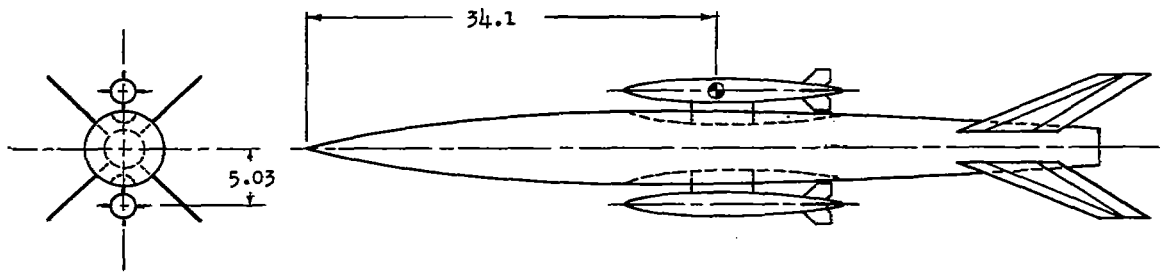


(e) Model E. Stores and cavities at X/L = 0.525 and pylon t/c = 0.06.

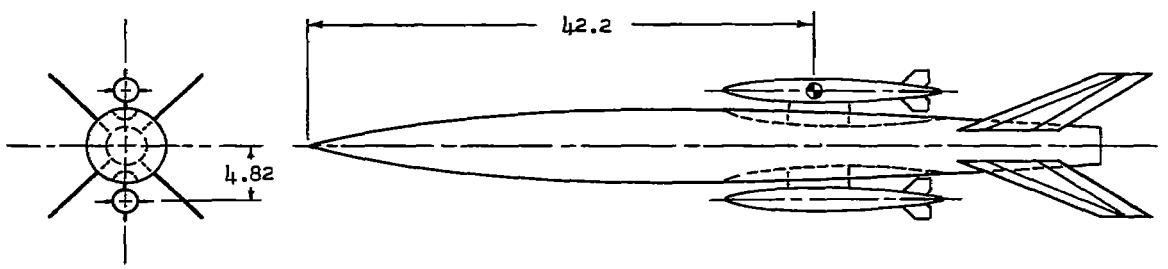


(f) Model F. Stores and cavities at X/L = 0.65 and pylon t/c = 0.06.

Figure 3.- Continued.

[redacted]

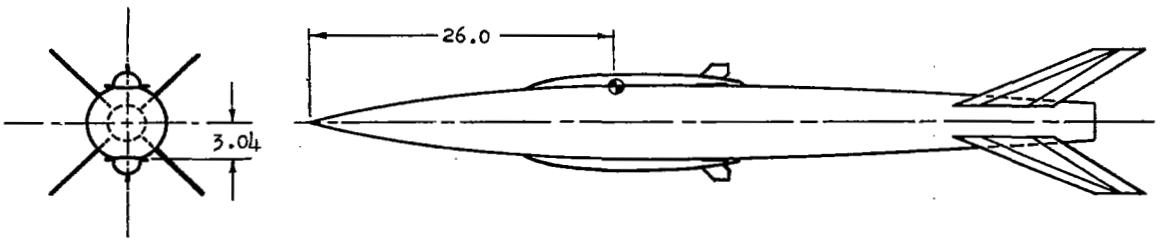


(g) Model G. Half-submerged stores at X/L = 0.40.

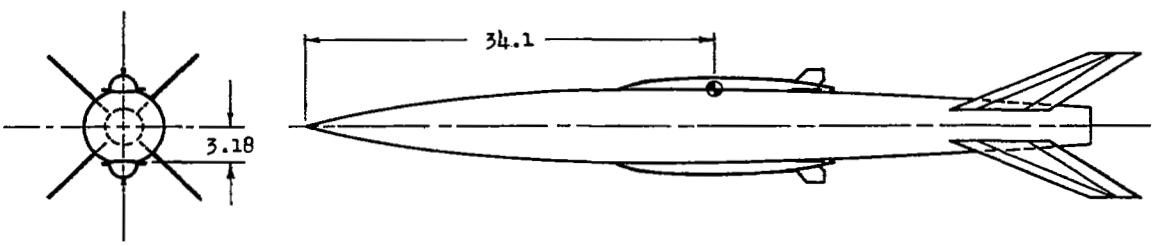


(h) Model H. Half-submerged stores at X/L = 0.525.

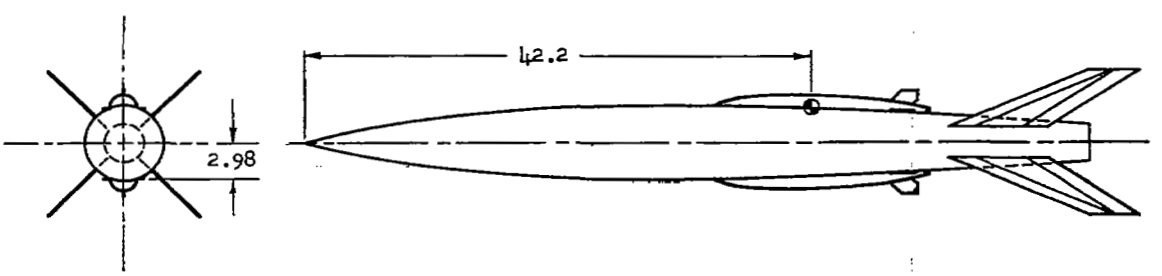


(i) Model I. Half-submerged stores at X/L = 0.65.

Figure 3.- Continued.

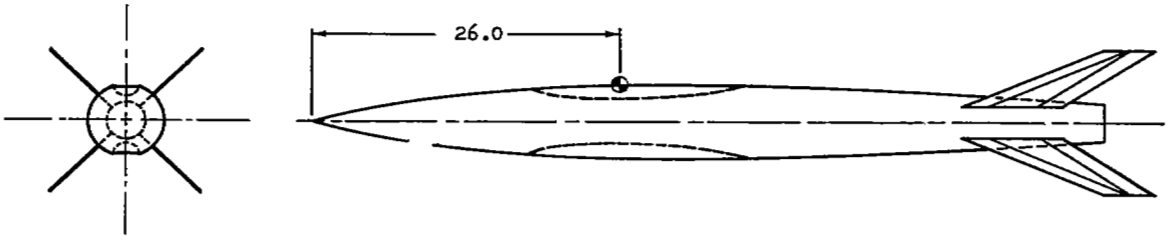


(j) Model J. Half-submerged-store cavities at X/L = 0.40.

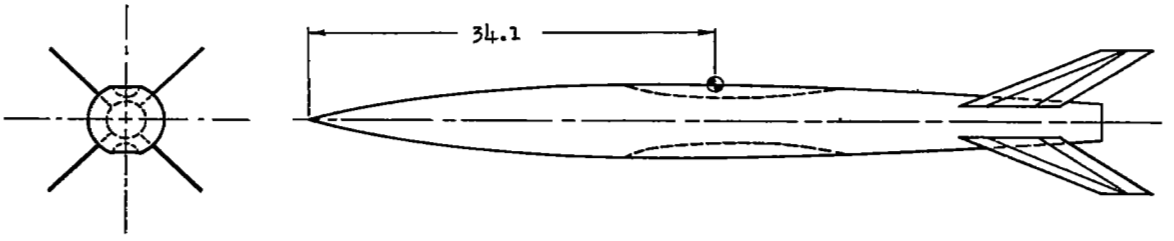


(k) Model K. Half-submerged-store cavities at X/L = 0.525.

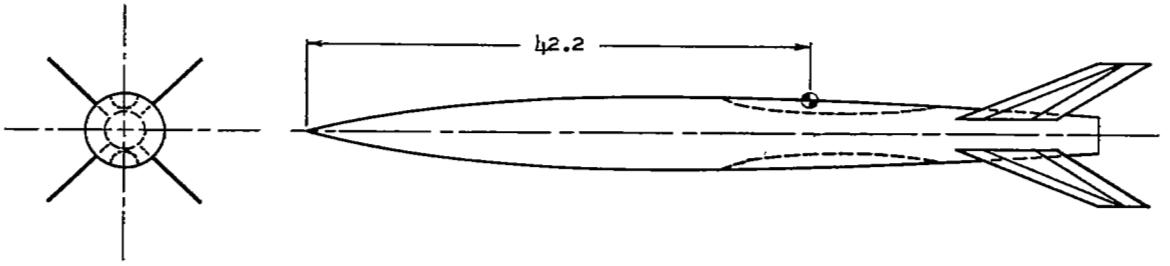


(l) Model L. Half-submerged-store cavities at X/L = 0.65.

Figure 3.- Concluded.

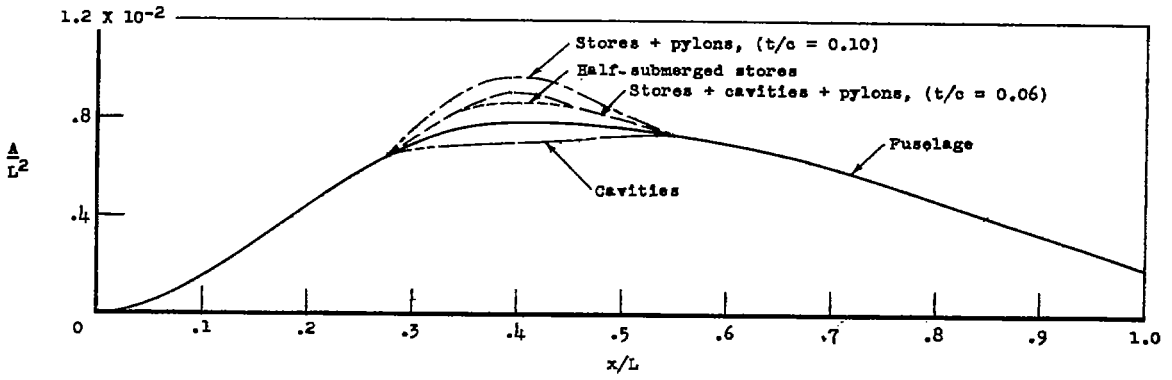


(a) Stores, cavities, and pylons at X/L = 0.40.

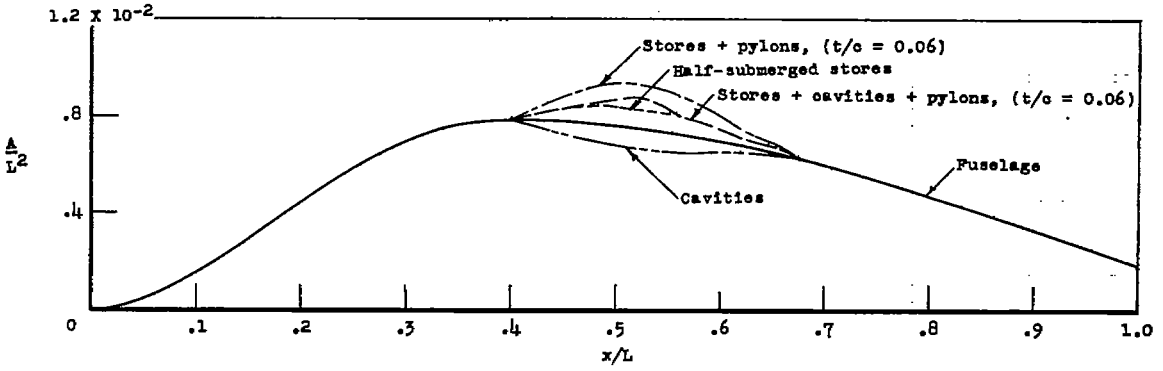


(b) Stores, cavities, and pylons at X/L = 0.525.

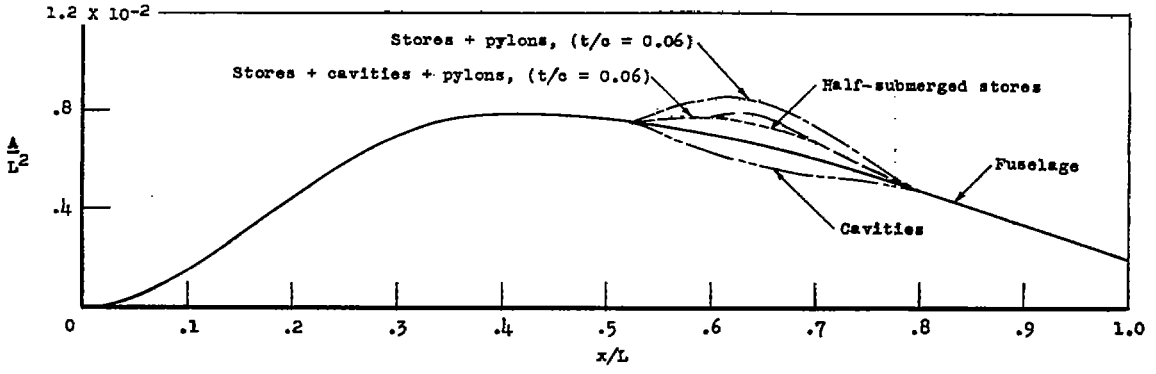


(c) Stores, cavities, and pylons at X/L = 0.65.

Figure 4.- Cross-sectional-area distribution of models tested.

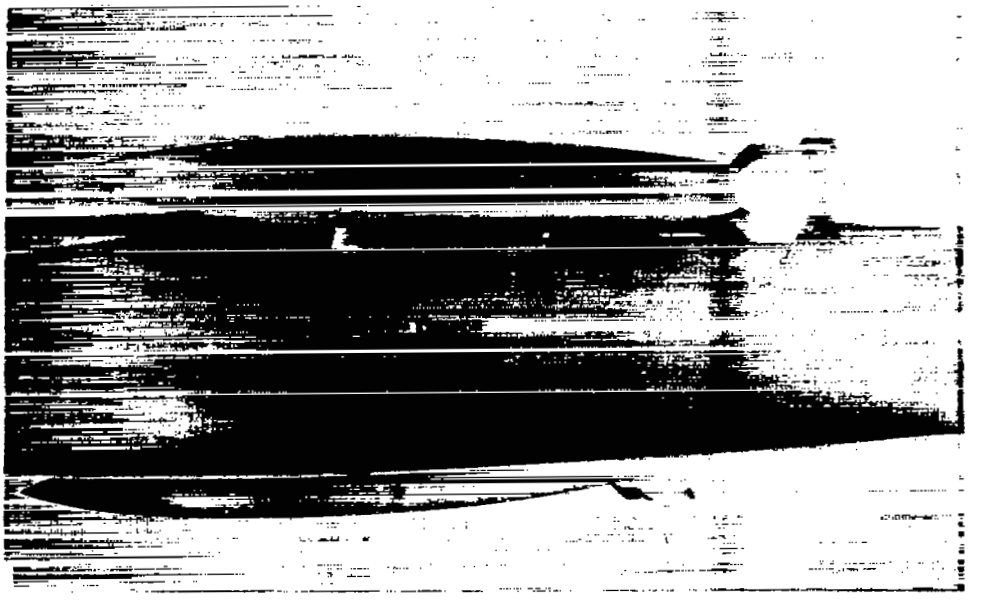

L-78719.1

(a) View of typical installation of pylon-mounted store.

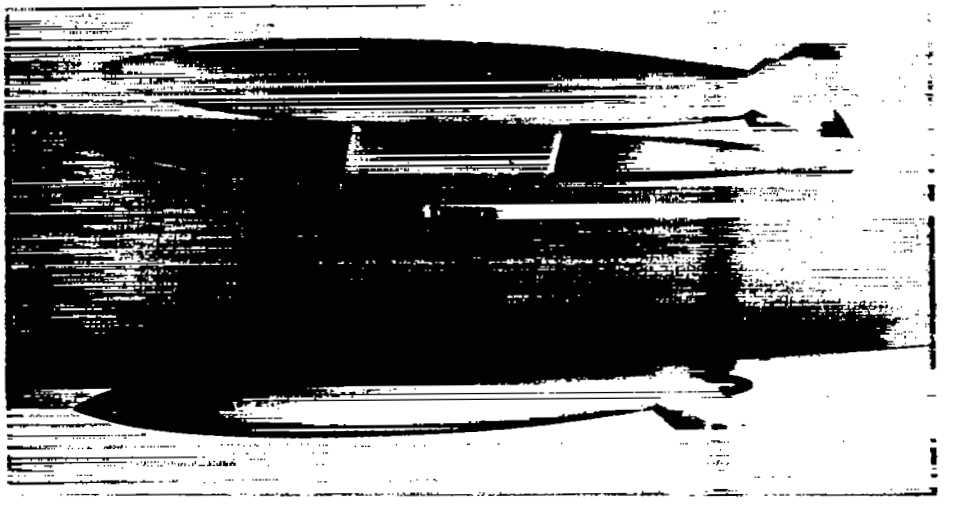

L-78715.1

(b) View of typical installation of pylon-mounted store and cavity.

Figure 5.- Photographs showing close-up views of stores, pylons, and cavities.

L-77840.1

(c) View of typical installation of half-submerged store.

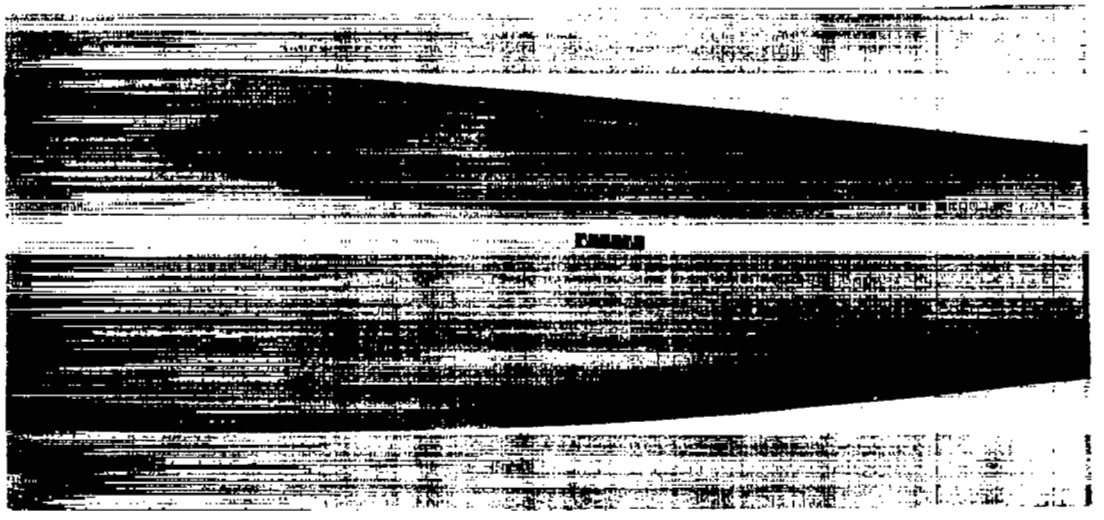

L-77817.1

(d) View of typical submerged half-store cavity in fuselage.

Figure 5.- Continued.

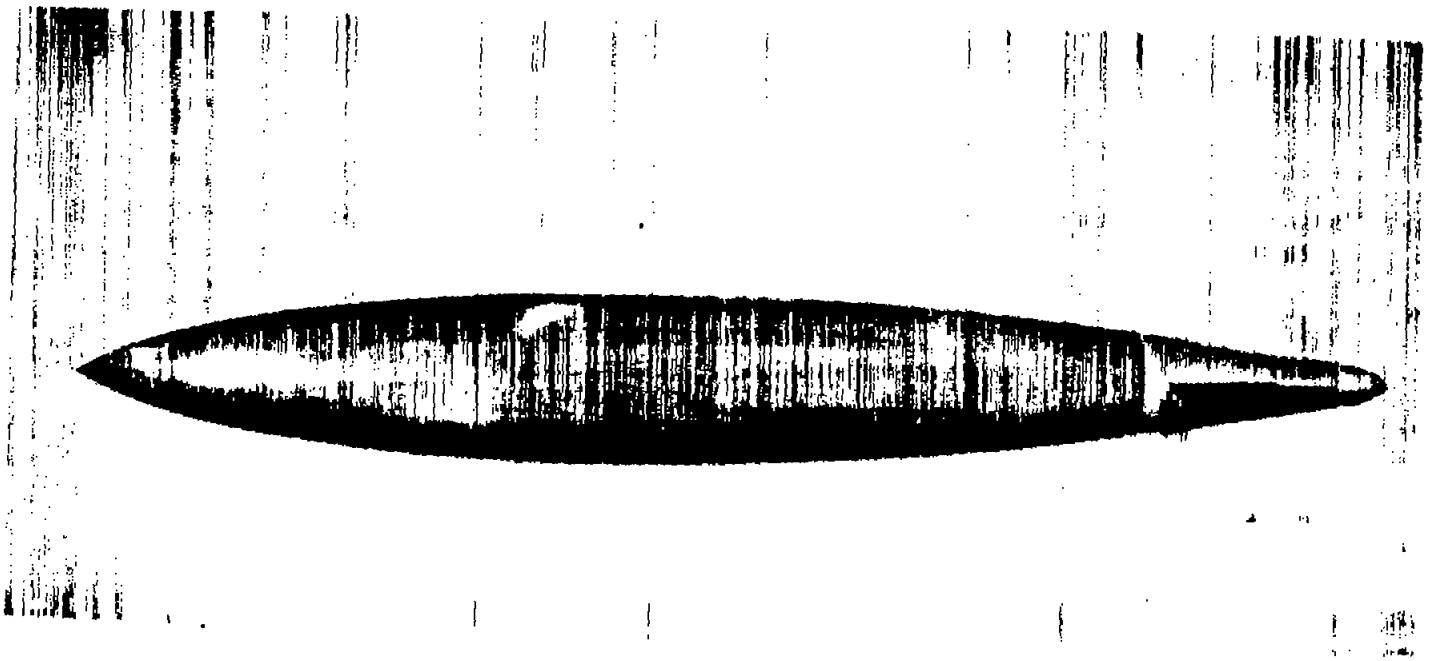

(e) Isolated store, Model N.

L-79118.1

Figure 5.- Continued.

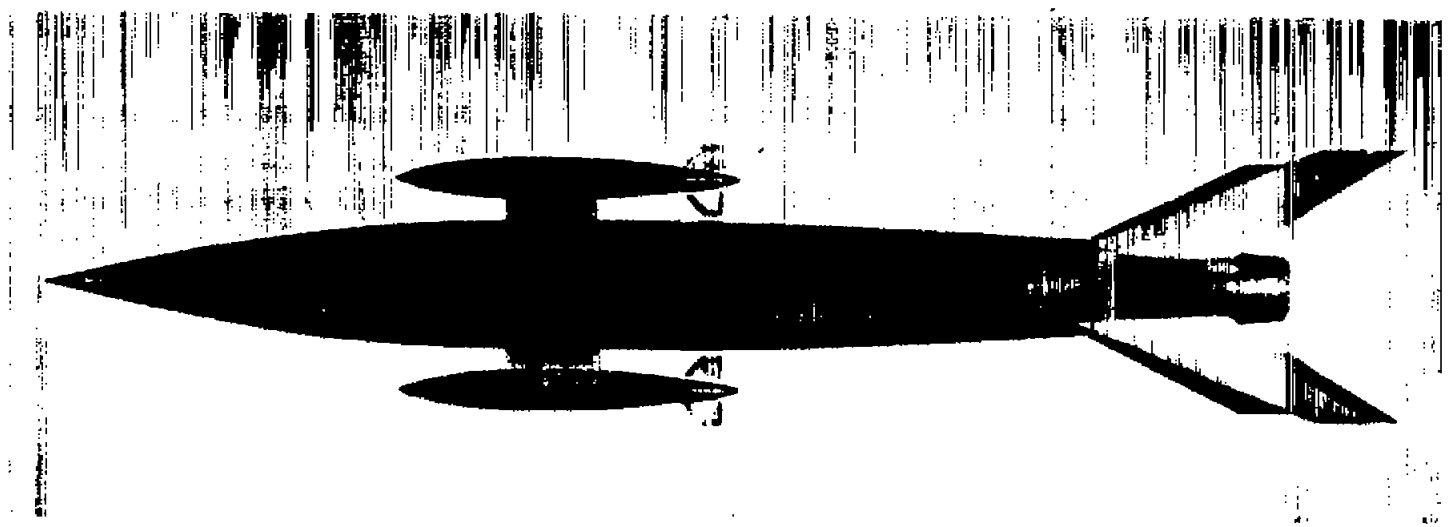

(f) View of typical model with pylon-mounted stores. L-76505.1

Figure 5.- Concluded.

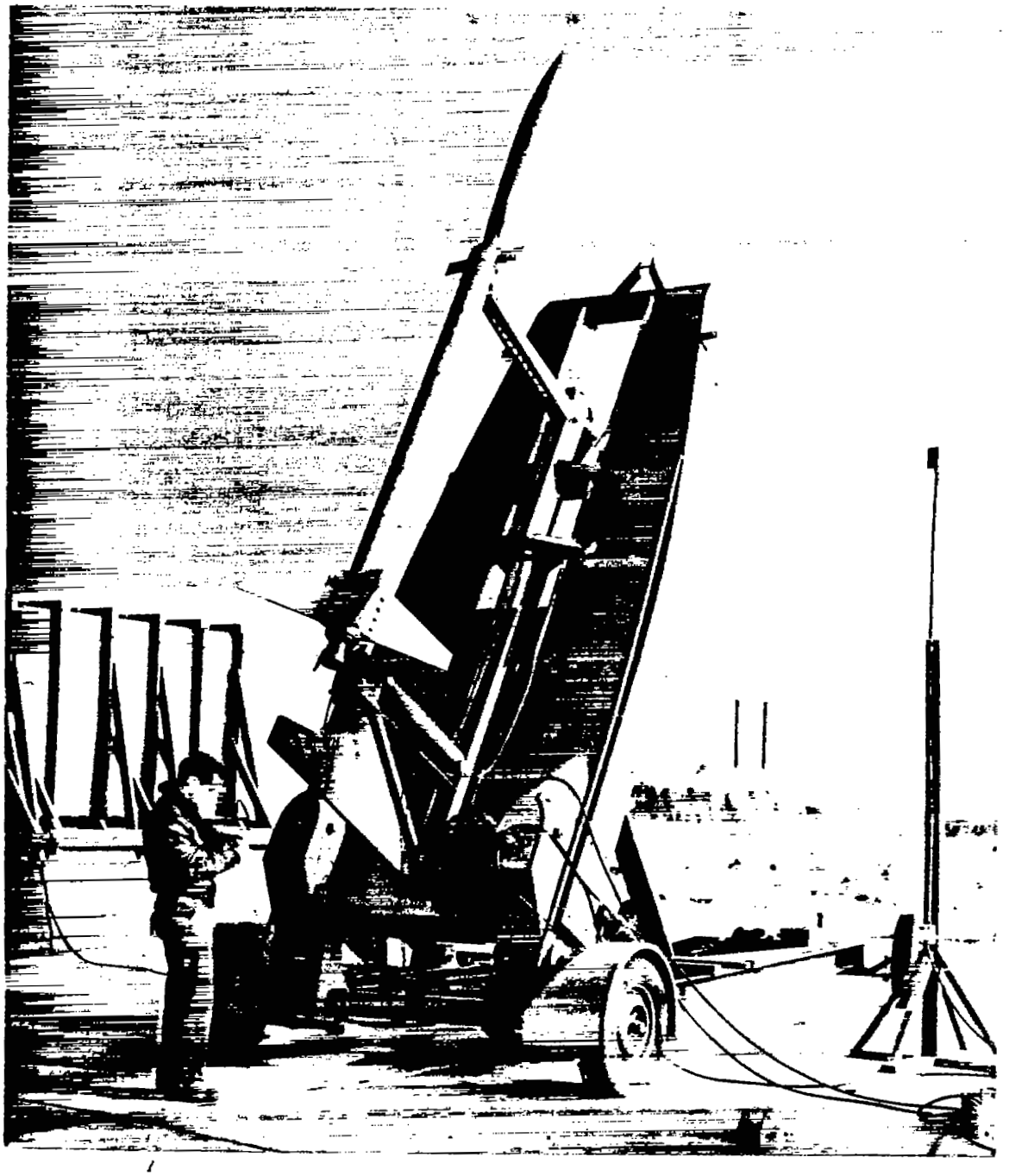

L-78108.1

Figure 6.- Parabolic fuselage (model 0) and booster on zero-length launcher.

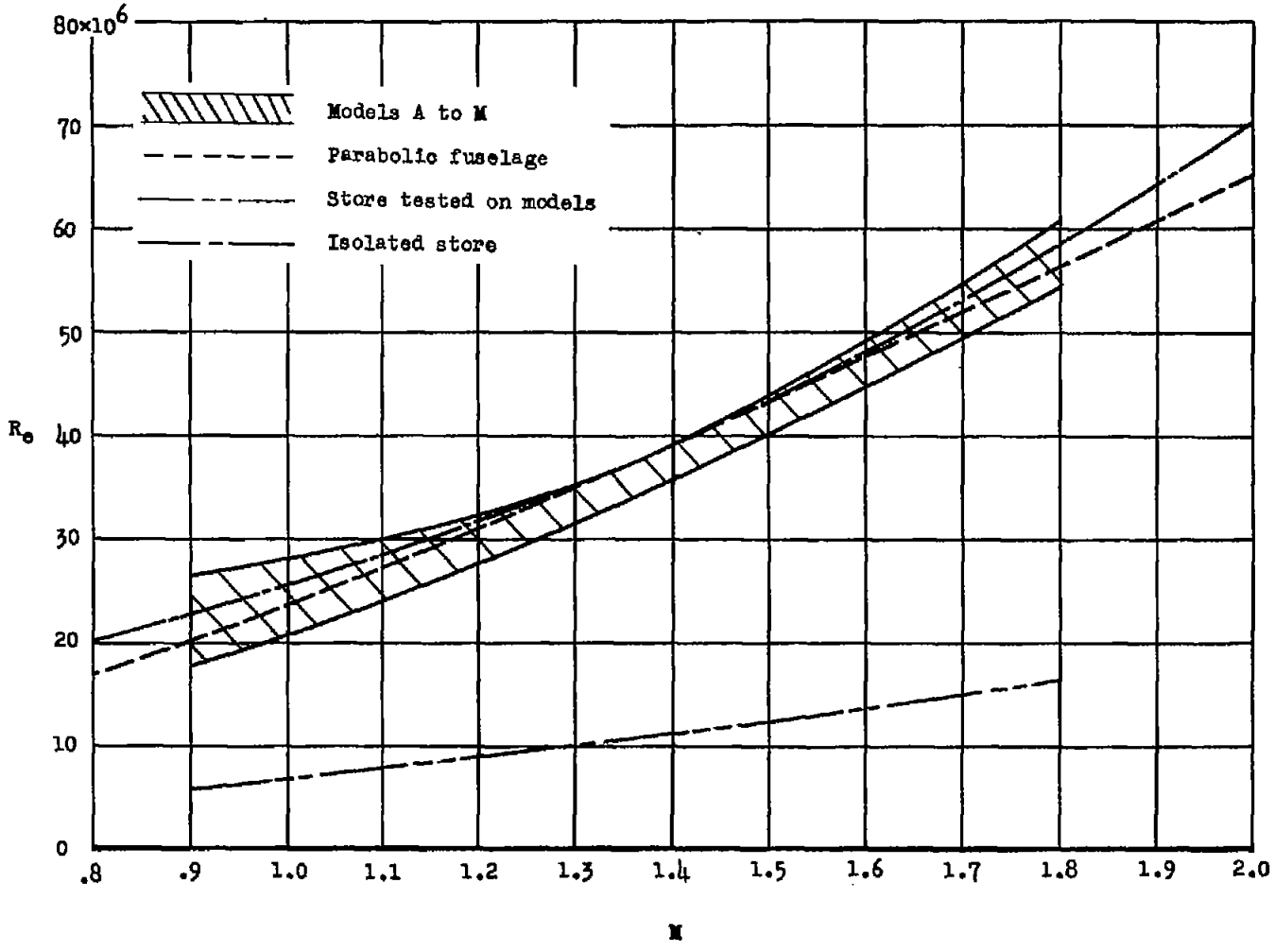


Figure 7.- Variations of Reynolds number with Mach number for models tested. Reynolds number is based on the length of the corresponding fuselage or store configuration.

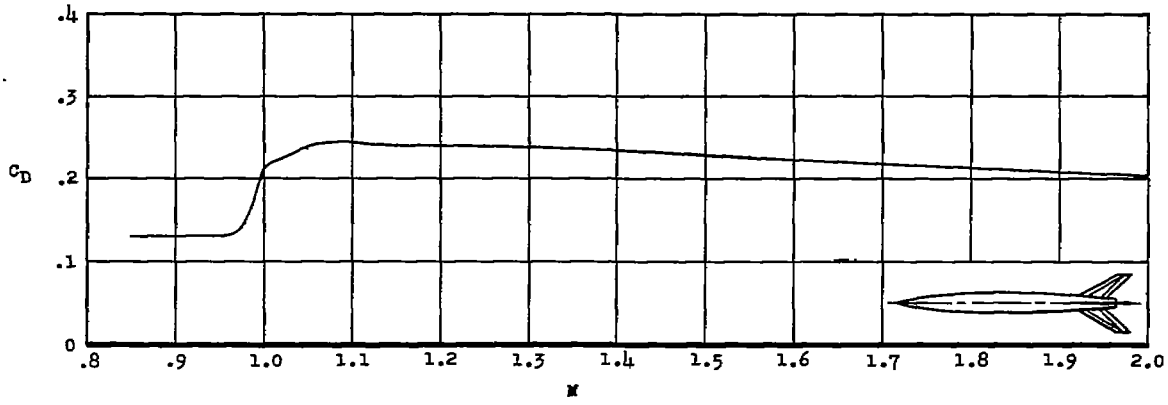


(a) Parabolic fuselage.

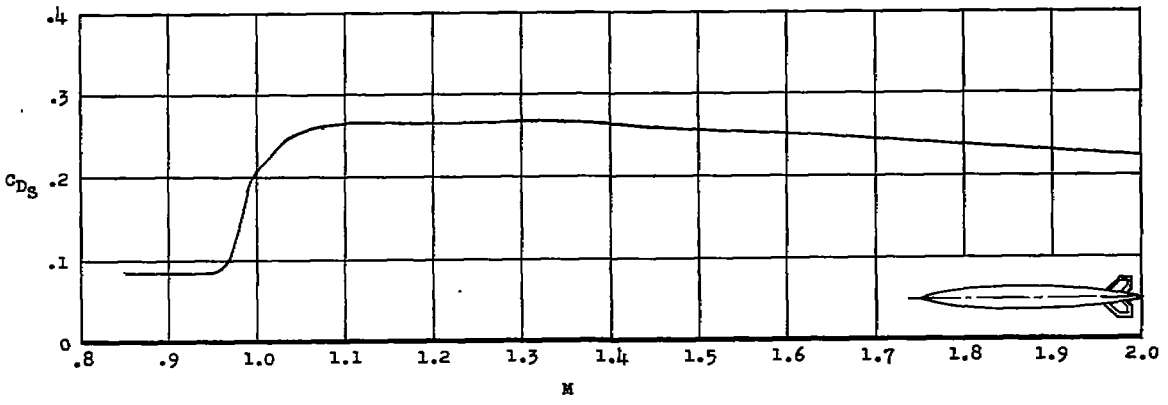


(b) Isolated store.

Figure 8.- Variations of drag coefficient with Mach number for the parabolic fuselage and the isolated store.

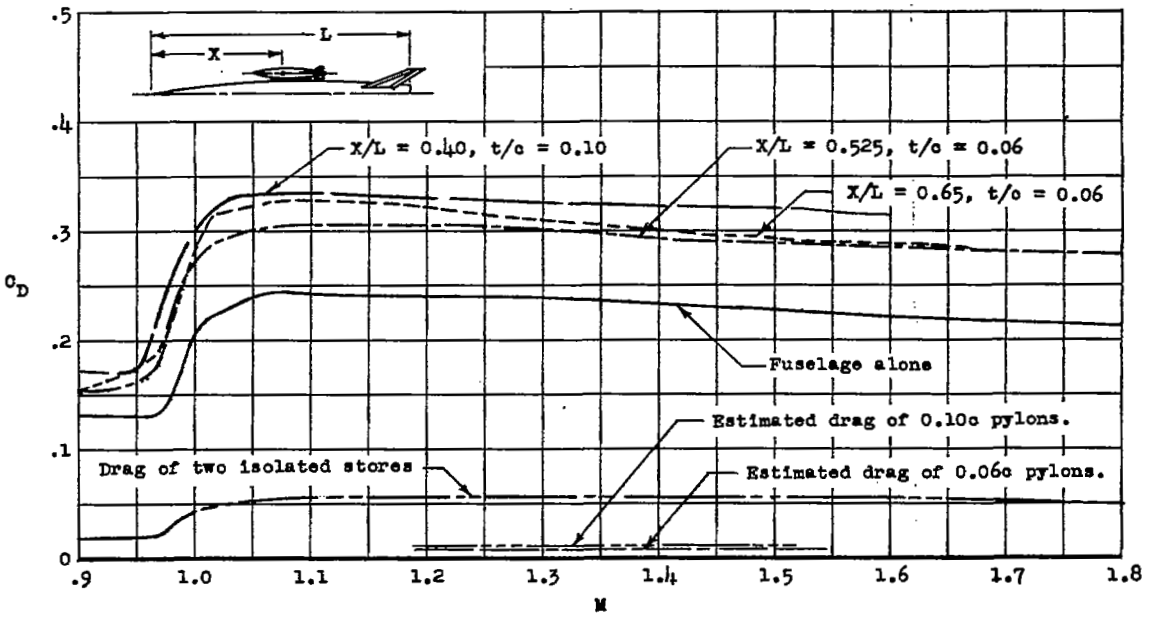


(a) Pylon-mounted stores.

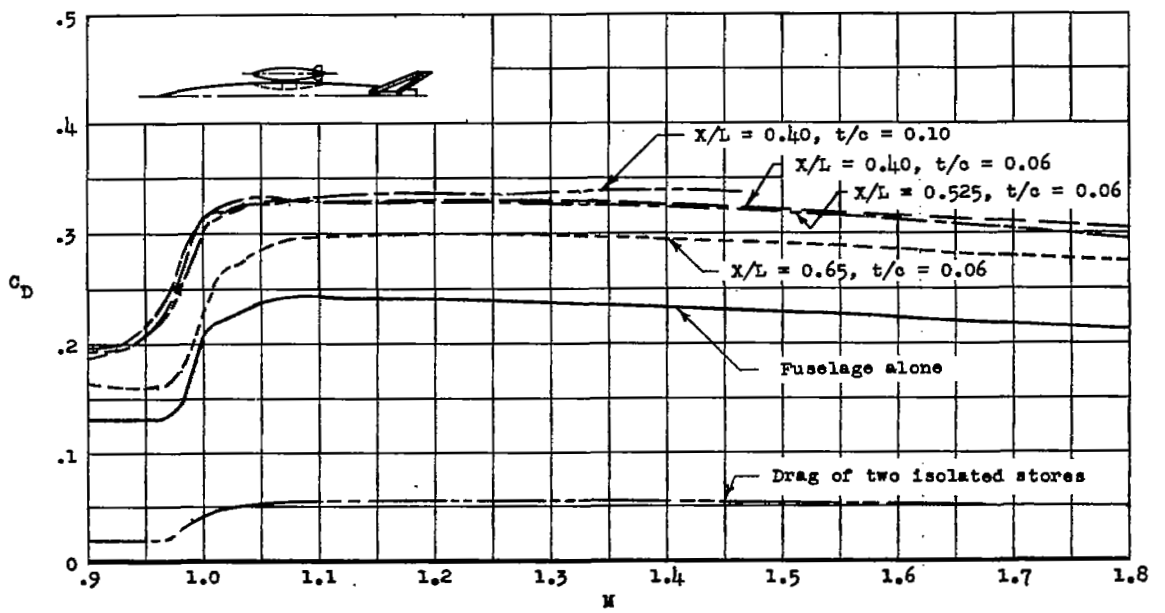


(b) Pylon-mounted stores and cavities.

Figure 9.- The effect on drag of longitudinal positioning of the symmetrically mounted stores, pylons, and cavities.

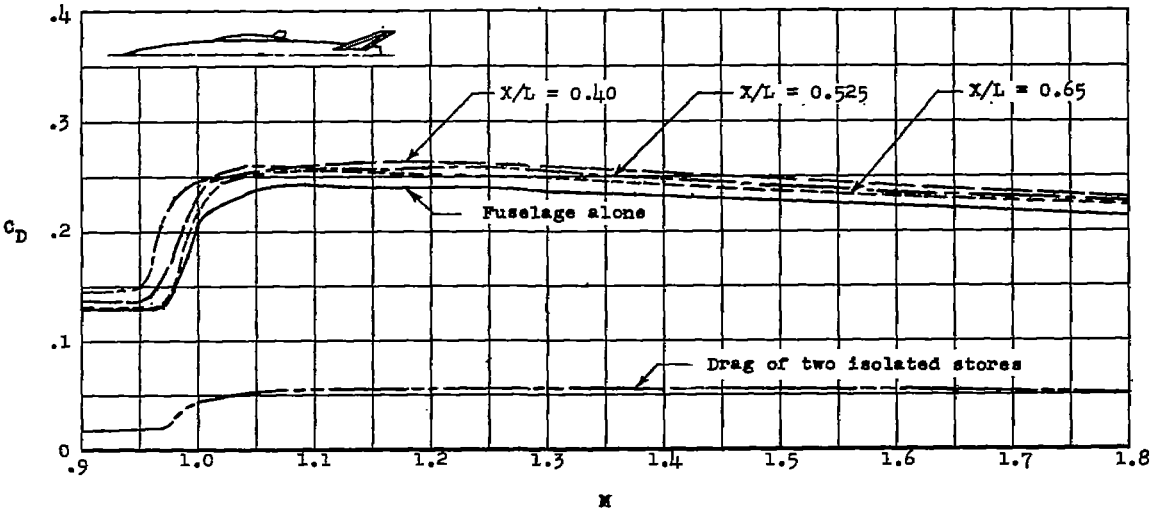


(c) Half-submerged stores.

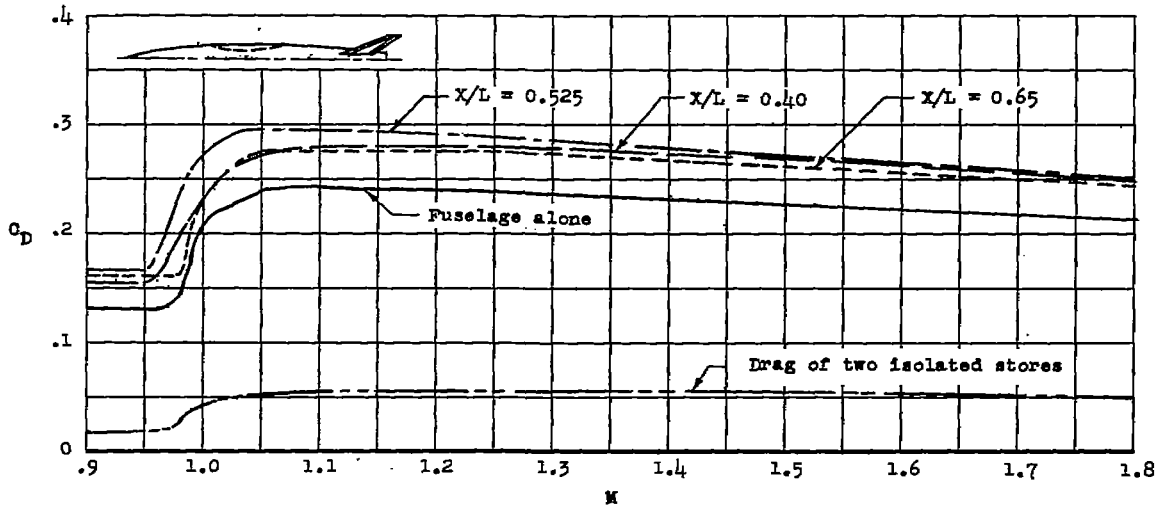


(d) Cavities.

Figure 9.- Concluded.

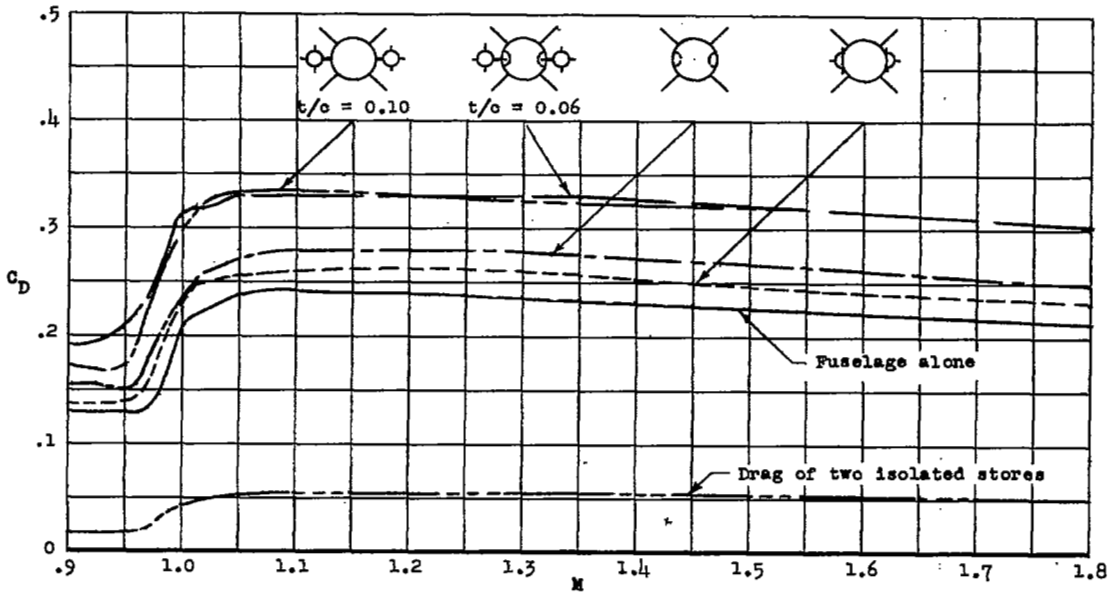


(a) X/L = 0.40.

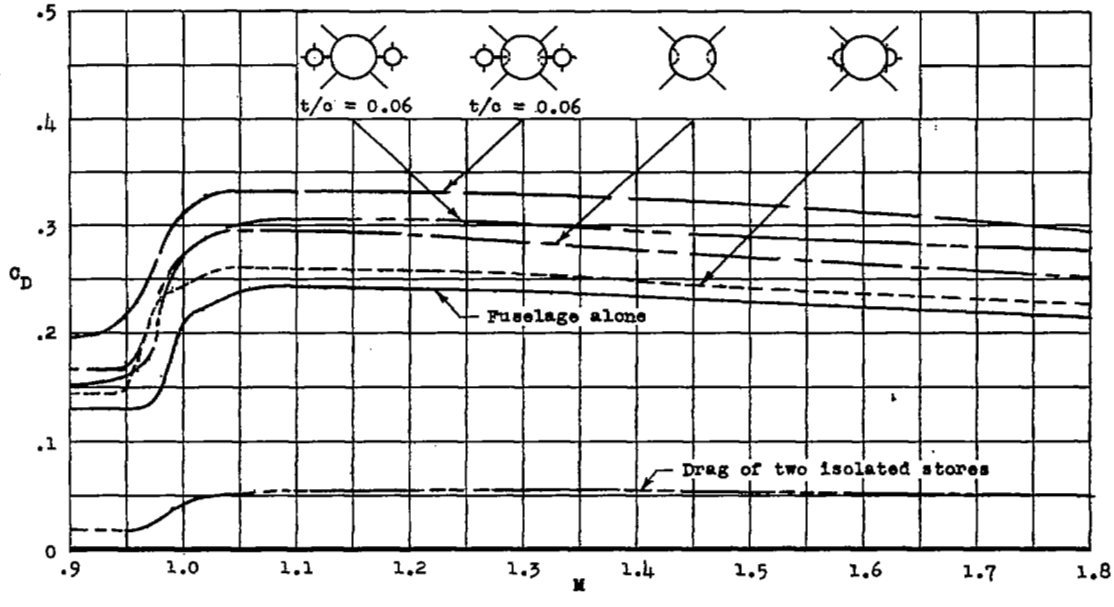


(b) X/L = 0.525.

Figure 10.- Comparisons of the variations of drag coefficient with Mach number for the configurations with the pylon-mounted stores, half-submerged stores, and cavities in symmetrical arrangements at each longitudinal location tested.

[redacted]

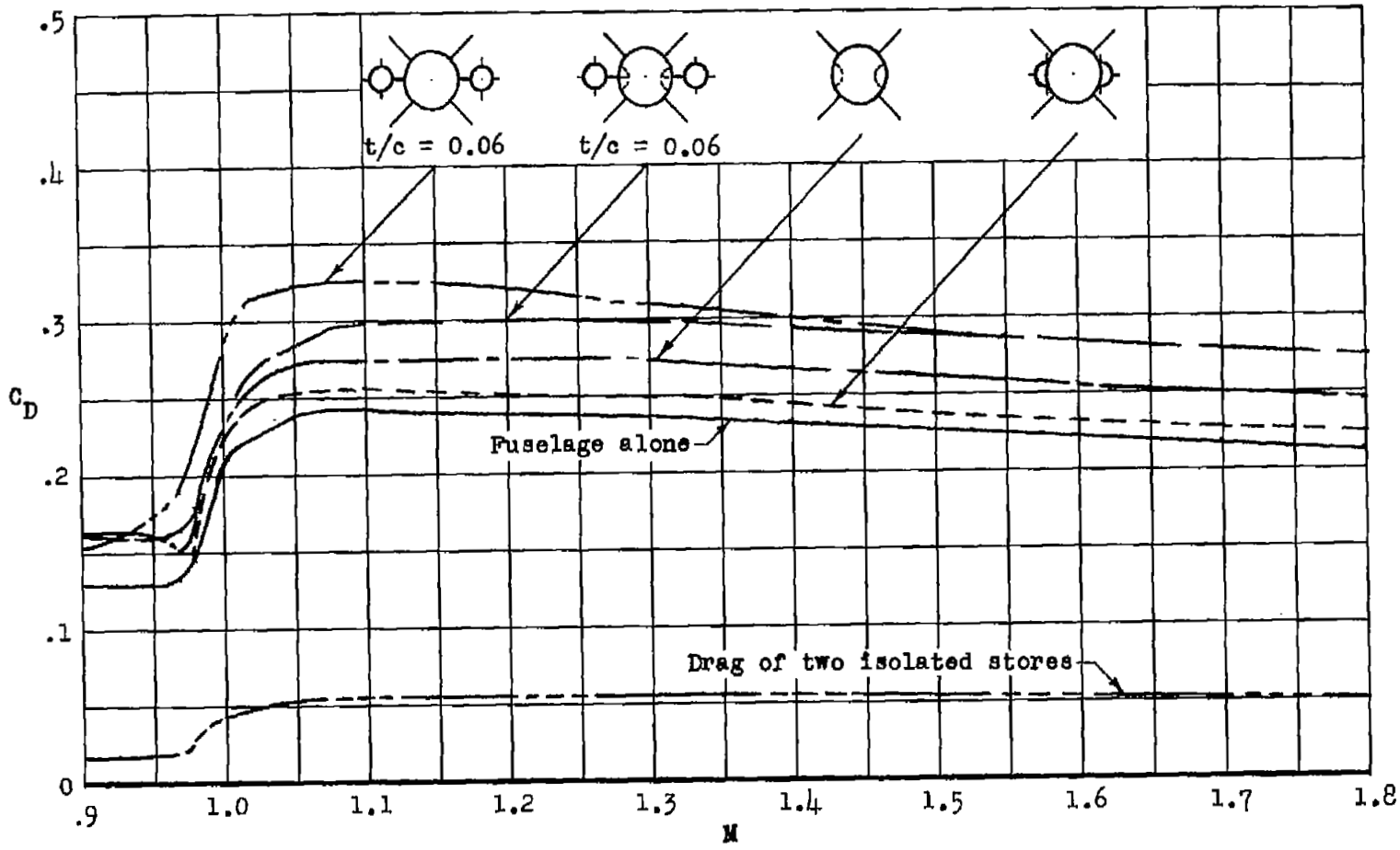


(c) X/L = 0.650.

Figure 10.- Concluded.

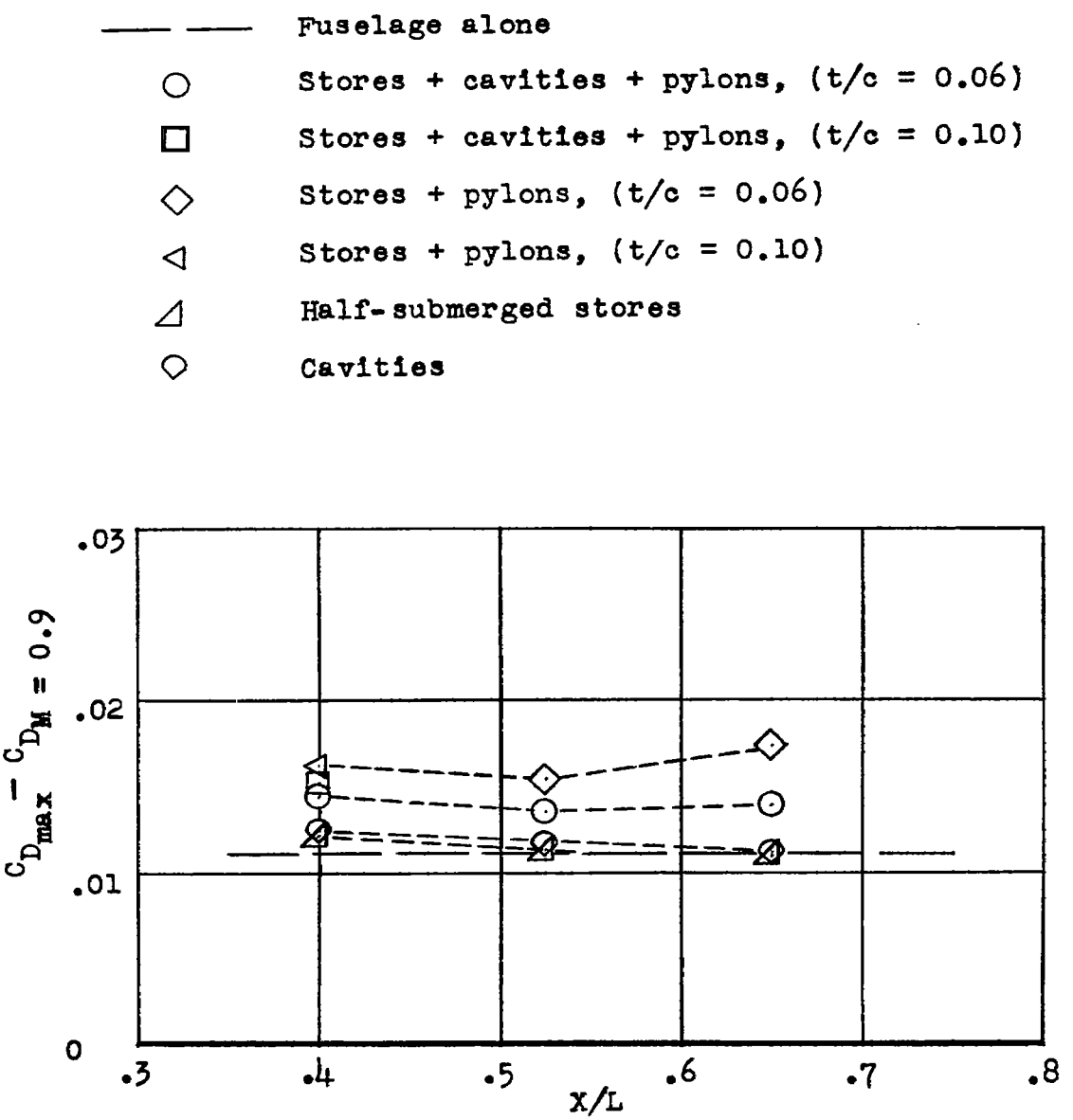


Figure 11.- Comparison of the maximum drag-rise coefficients of the models tested.

[redacted]

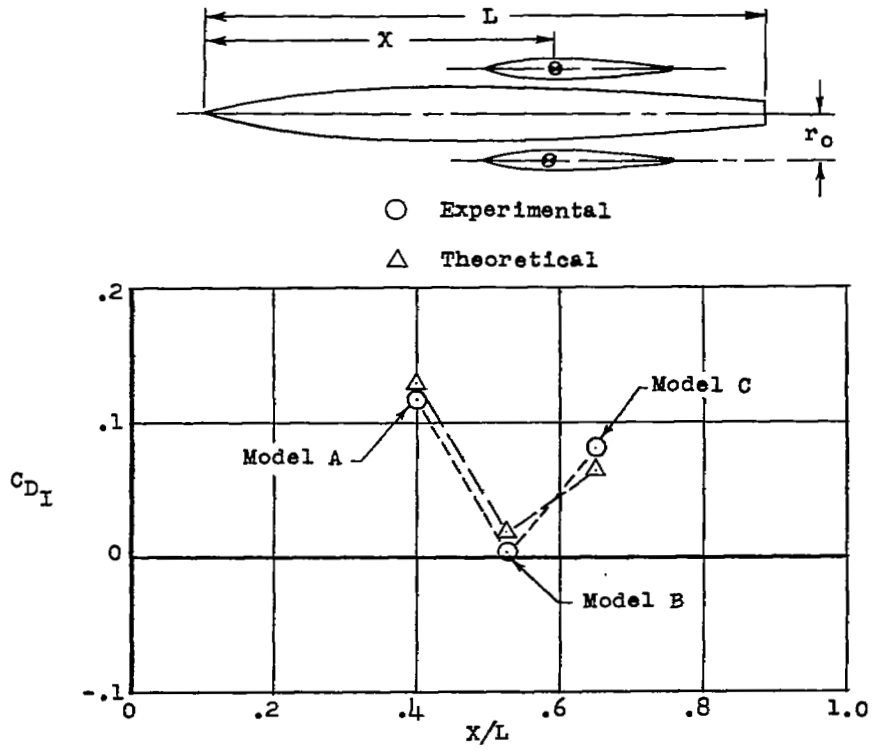


(a) M = 1.2.

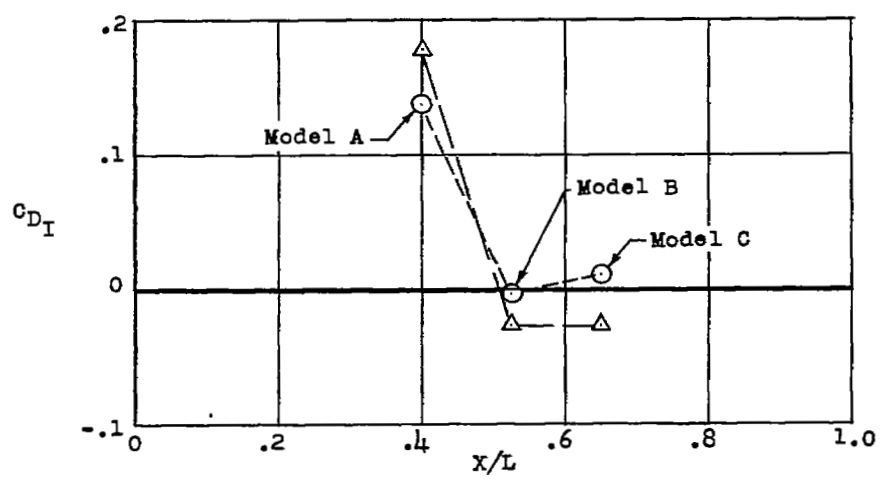


(b) M = 1.5.

Figure 12.- Comparisons of the experimental and theoretical interference drag coefficients for the symmetrically mounted store arrangements of models A, B, and C.

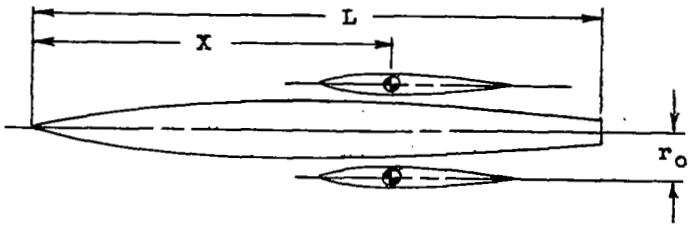


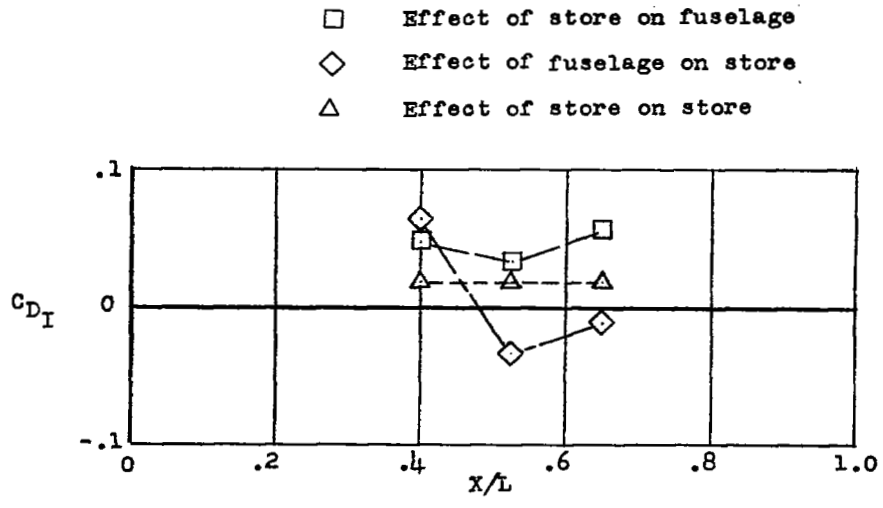


(a) M = 1.2.

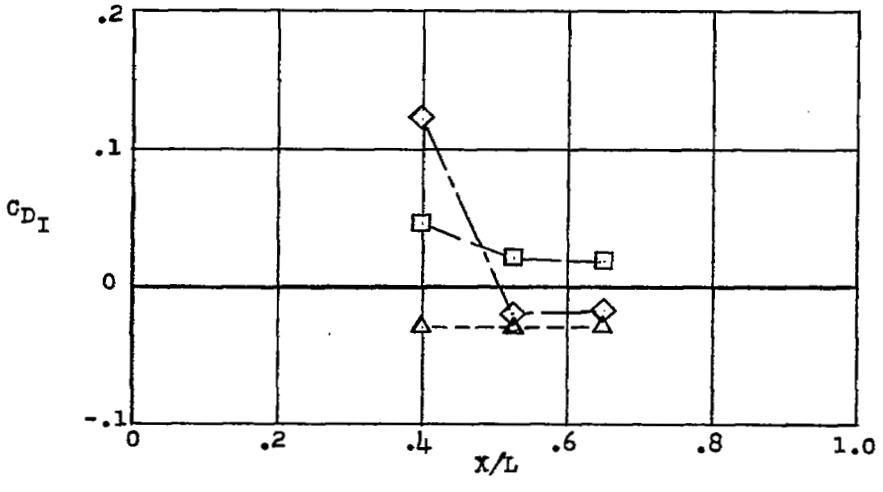


(b) M = 1.5.

Figure 13.- Comparisons of the theoretical interference drag coefficients for the principal components of models A, B, and C.

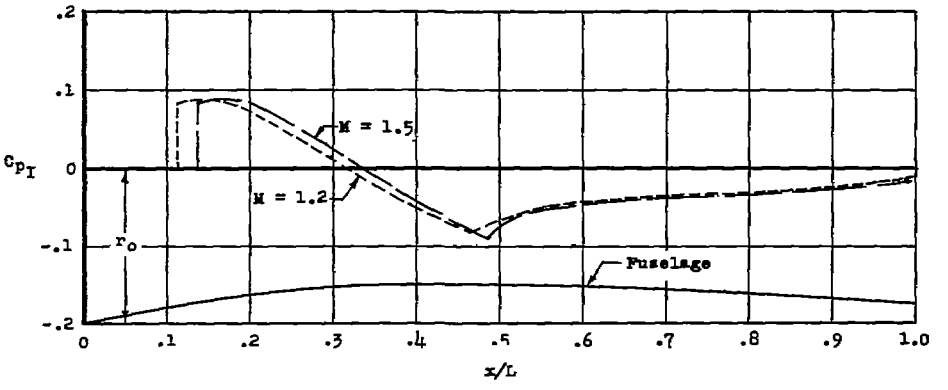


(a) Pressure distribution in flow field of fuselage at the location of the store axes.

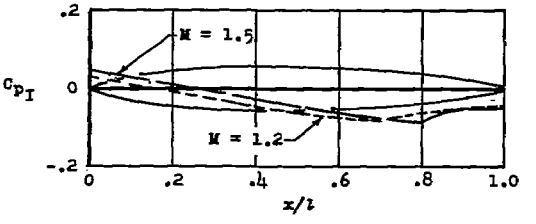


(b) Interference pressures acting on store at X/L = 0.40. Model A.

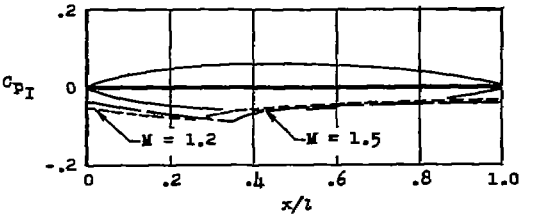


(c) Interference pressures acting on store at X/L = 0.525. Model B.

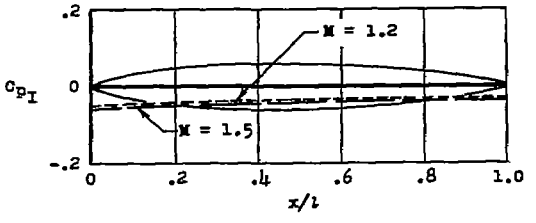


(d) Interference pressures acting on store at X/L = 0.65. Model C.

Figure 14.- Theoretical interference pressure coefficients from fuselage acting on the symmetrically mounted stores of models A, B, and C.

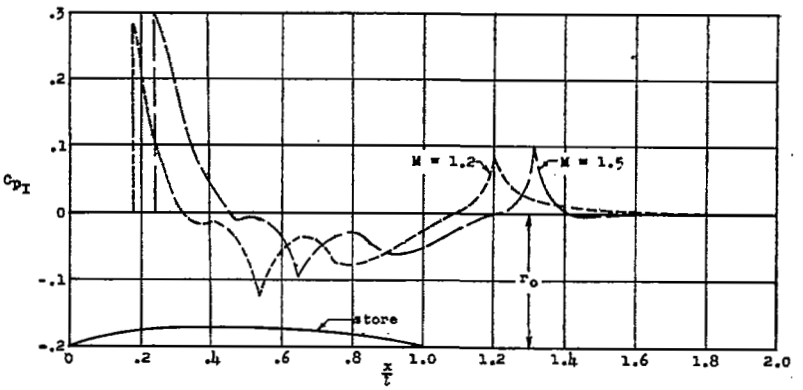


(a) Pressure distribution in flow field of store at the location of the fuselage axis.

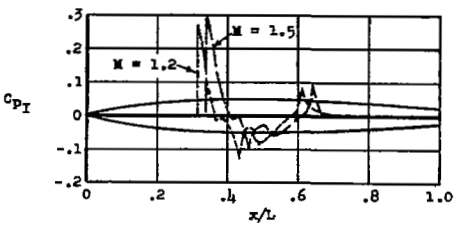


(b) Interference pressures acting on fuselage from store at X/L = 0.40. Model A.

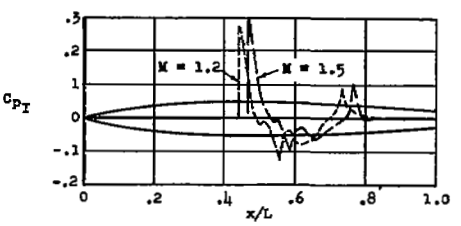


(c) Interference pressures acting on fuselage from store at X/L = 0.525. Model B.

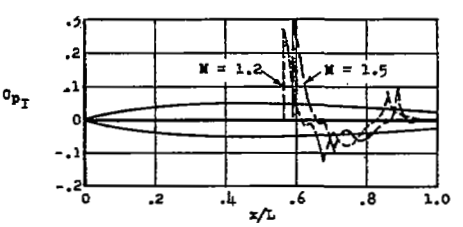


(d) Interference pressures acting on fuselage from store at X/L = 0.65. Model C.

Figure 15.- Theoretical interference pressure coefficients from symmetrically mounted stores acting on the fuselage of models A, B, and C.

[redacted]

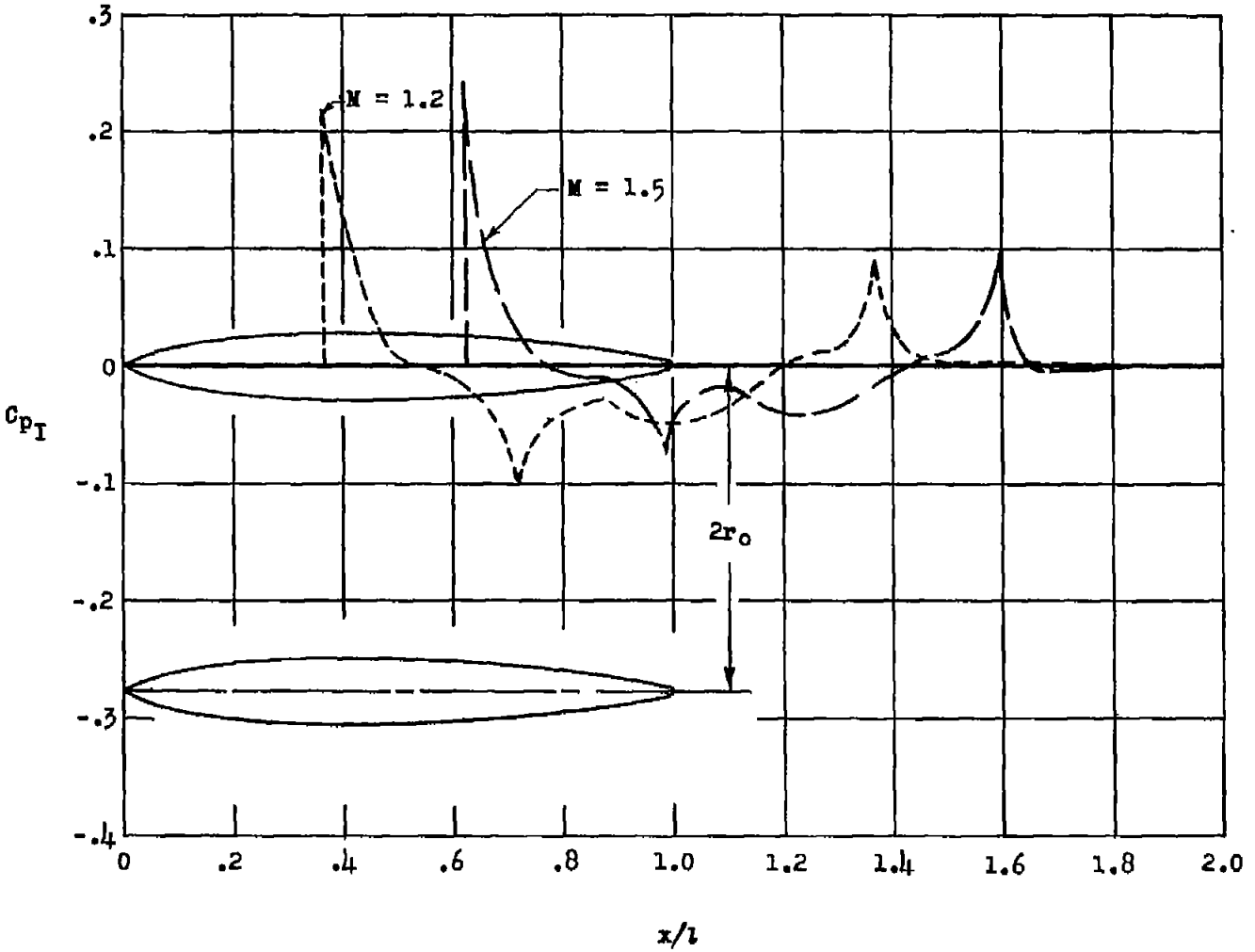


Figure 16.- Theoretical interference pressure coefficients induced from one store on the neighboring store for the symmetrically mounted stores of models A, B, and C.